
FairNorm: Fair and Fast Graph Neural Network Training

O. Deniz Kose

Department of Electrical Engineering and Computer Science
University of California, Irvine
okose@uci.edu

Yanning Shen

Department of Electrical Engineering and Computer Science
University of California, Irvine
yannings@uci.edu

Abstract

Graph neural networks (GNNs) have been demonstrated to achieve state-of-the-art for a number of graph-based learning tasks, which leads to a rise in their employment in various domains. However, it has been shown that GNNs may inherit and even amplify bias within training data, which leads to unfair results towards certain sensitive groups. Meanwhile, training of GNNs introduces additional challenges, such as slow convergence and possible instability. Faced with these limitations, this work proposes FairNorm, a unified normalization framework that reduces the bias in GNN-based learning while also providing provably faster convergence. Specifically, FairNorm employs fairness-aware normalization operators over different sensitive groups with learnable parameters to reduce the bias in GNNs. The design of FairNorm is built upon analyses that illuminate the sources of bias in graph-based learning. Experiments on node classification over real-world networks demonstrate the efficiency of the proposed scheme in improving fairness in terms of statistical parity and equal opportunity compared to fairness-aware baselines. In addition, it is empirically shown that the proposed framework leads to faster convergence compared to the naive baseline where no normalization is employed.

1 Introduction

Graphs are powerful structures in modeling complex systems and the relations within them. Hence, they are widely employed to represent various real-world systems, such as gene networks, traffic networks and social networks to name a few. Such expressiveness has led to a rise in the attention towards learning over graphs, and it has been shown that graph neural networks (GNNs) achieve the state-of-the-art for several tasks over graphs [1, 2, 3, 4, 5, 6]. GNNs create node representations by repeatedly aggregating information from the neighbors, which can be employed on ensuing tasks such as traffic forecasting [7], crime forecasting [8], and recommendation systems [9].

Due to their success, machine learning (ML) models have widespread use in our everyday lives to make life-changing decisions, which makes it essential to prevent any discriminatory behaviour in these models towards under-represented groups. However, several studies have demonstrated that ML models propagate the historical bias within the training data [10, 11] and lead to discriminative results in ensuing applications. Particular to GNNs, it has been shown that in addition to propagating the already existing bias, GNN-based learning may even amplify it due to the utilization of biased graph topologies [12]. This well-motivates the studies in fairness-aware GNN-based learning.

Normalization operations are introduced to shift and scale the hidden representations created in deep neural networks (DNNs) in order to accelerate the optimization process in training [13, 14, 15, 16, 17, 18, 19, 20]. While the other aspects of GNN-based learning are theoretically investigated, such as generalization [21, 22], expressiveness [23, 24, 25], the optimization of GNNs is analytically an under-explored area. Practically, training GNNs generally has a slow convergence rate and is accompanied by instability issues [23]. Inspired by this, [26] investigates the effect of a shift operation on a simple GNN-based learning environment and proposes a normalization framework that is suitable for GNNs. The proposed framework, GraphNorm [26], is demonstrated to be more effective in improving convergence speed over graphs compared to previously presented normalization strategies in other domains.

It has been shown in [27] that the distribution discrepancy among different sensitive groups is one of the leading factors to bias in general ML algorithms. For GNNs, fairness analyses have also shown that the distributions of the representations of different sensitive groups affect the resulting bias [28, 29]. In the meantime, normalization layers learn the parameters that manage the sample mean and variance of these hidden representations. Herein, we emphasize that the normalization layer inherently provides an ability to manipulate said parameters in order to mitigate bias, while also improving the convergence. Motivated by this, this study proposes a unified framework that mitigates bias in GNN-based learning, while also providing a faster convergence through the employment of a normalization layer. Overall, our contributions in this paper can be summarized as follows:

c1) We propose a framework that can reduce bias while providing a higher convergence speed for a GNN-based learning environment. To the best of our knowledge, FairNorm is the first attempt to improve fairness and convergence speed in a unified framework.

c2) The effect of the fairness-aware shift operations on convergence rate is investigated in a simple GNN-based learning framework. It is analytically demonstrated that the proposed shift operations can improve the convergence rate for node classification compared to the case where no shift is employed.

c3) For fairness considerations, two fairness-aware regularizers are introduced for the trainable parameters of normalization layers. The designs of said regularizers are based on the theoretical understanding regarding the sources of bias in GNN-based learning.

c4) Empirical results are obtained over real-world networks in terms of utility and fairness metrics for node classification. It is demonstrated that compared to fairness-aware baselines, FairNorm leads to an improvement in fairness metrics while providing comparable utility. Meanwhile, it is shown that applying FairNorm enhances the convergence speed with respect to the no-normalization baseline.

2 Related Work

Fairness-aware learning over graphs: In fairness-aware learning over graphs, [30] serves as a seminal work based on random walks. In addition, [12, 31, 32] propose to use adversarial regularization to reduce bias in GNNs. Another approach is to utilize a Bayesian approach where the sensitive information is modeled in the prior distribution to enhance fairness over graphs [33]. Furthermore, [34] performs a PAC-Bayesian analysis and links the notion of subgroup generalization to accuracy disparity, and [35] proposes several strategies including GNN-based ones to reduce bias for the representations of heterogeneous information networks. Specifically for fairness-aware link prediction, while [36] introduces a regularizer, [28, 37] propose strategies that alter the adjacency matrix. With a specific consideration of individual fairness over graphs, [38] proposes a ranking-based framework. Another research direction in fairness-aware graph-based learning is to modify the graph structure to combat bias resulted from the graph connectivity [39, 40, 29, 41]. Differing from all previous works, the proposed framework herein proposes a unified framework that can mitigate bias in GNN-based learning together with an enhanced convergence speed.

Normalization: Batch Normalization (BatchNorm) [13] is the pioneering study that proposes to shift and scale the hidden representations in a batch to accelerate the convergence of training for DNNs. As a following work, Instance Normalization (InstanceNorm) [14] is proposed for real-time image generation, which applies normalization over individual images instead of the samples in a batch. For permutation-equivalent data processing, adaptations of InstanceNorm [42, 43] have also been presented. Specifically for GNNs, [23] employs BatchNorm within the framework of graph isomorphism networks, while a prior version of [44] normalizes node features based on the graph size. A size-agnostic normalization for graphs, GraphNorm [26], is further proposed, which improves

InstanceNorm for graphs with a learnable shift to prevent degradation in expressiveness. However, none of the aforementioned normalization schemes consider fairness.

3 Preliminaries

This study develops a unified training scheme for GNNs that can improve fairness while at the same time enhance the convergence speed, given an input graph $\mathcal{G} := (\mathcal{V}, \mathcal{E})$, where $\mathcal{V} := \{v_1, v_2, \dots, v_N\}$ denotes the node set, and $\mathcal{E} \subseteq \mathcal{V} \times \mathcal{V}$ is the edge set. Matrices $\mathbf{X} \in \mathbb{R}^{F \times N}$ and $\mathbf{A} \in \{0, 1\}^{N \times N}$ are the feature and adjacency matrices, respectively, where $\mathbf{A}_{ij} = 1$ if and only if $(v_i, v_j) \in \mathcal{E}$. Degree matrix $\mathbf{D} \in \mathbb{R}^{N \times N}$ is defined to be a diagonal matrix with the n th diagonal entry denoting the degree of node v_n . In this study, the sensitive attributes of the nodes are denoted by $\mathbf{s} \in \{0, 1\}^{N \times 1}$, where the existence of a single, binary sensitive attribute is considered. Furthermore, \mathcal{S}^0 and \mathcal{S}^1 denote the set of nodes whose sensitive attributes are 0 and 1, respectively. Node representations at k th layer are represented by $\mathbf{H}^{(k)} \in \mathbb{R}^{F \times N}$, where \mathbf{h}_j denotes the representation of node v_j and $h_{i,j}$ is the i th feature of \mathbf{h}_j . Vectors $\mathbf{x}_j \in \mathbb{R}^F$ and $s_j \in \{0, 1\}$ will be used to denote the feature vector and the sensitive attribute of node v_j . Throughout the paper, $\max(\cdot, \dots, \cdot)$ outputs the element-wise maximum vector of its argument vectors, and $\text{mean}(\cdot, \dots, \cdot)$ denotes the sample mean operator.

GNNs produce node embeddings by repeatedly aggregating information from neighbors. Different GNN structures that are based on different aggregation strategies are proposed so far [4, 5, 23]. A general formulation of GNNs in matrix form follows as:

$$\mathbf{H}^{(k)} = \text{Act} \left(\mathbf{W}^{(k)} \mathbf{H}^{(k-1)} \mathbf{Q} \right)$$

where $\mathbf{W}^{(k)}$ represents the weight matrix of GNN at k th layer and Act denotes activation function. In this formulation, \mathbf{Q} matrix specifies the information aggregation process from neighbors, which changes in different GNN frameworks. For example, $\mathbf{Q} = \hat{\mathbf{D}}^{-\frac{1}{2}} \hat{\mathbf{A}} \hat{\mathbf{D}}^{-\frac{1}{2}}$ for Graph Convolutional Networks (GCN) [4], where $\hat{\mathbf{A}} = \mathbf{A} + \mathbf{I}_N$ with $\mathbf{I}_N \in \{0, 1\}^{N \times N}$ denoting the identity matrix, and $\hat{\mathbf{D}}$ is the degree matrix corresponding to $\hat{\mathbf{A}}$. Finally, the representations created after one aggregation process are denoted by $\mathbf{Z}^{(k)} = \mathbf{H}^{(k-1)} \mathbf{Q}$. Note that the superscript (k) for layer number is dropped in the remaining of the paper, as the proposed framework is applicable to every layer in the same way.

3.1 Normalization for GNNs

For deep neural networks (DNNs), normalization methods have been shown to accelerate training through shifting and scaling the hidden representations [13, 14, 15, 16, 17, 18, 19, 20]. Normalization methods differ in the set of features over which the normalization is applied. For example, Layer normalization (LayerNorm) normalizes the feature vectors at each instance in a sequence [15], while BatchNorm executes the normalization over individual features across different samples in a batch. In general, different normalization methods are proposed for different domains, and there is not a universal normalization strategy that suits every domain [26]. For example, while LayerNorm is presented for natural language processing [15], InstanceNorm seeks specifically to improve the optimization for style transfer tasks [14]. For GNNs, [26] demonstrates that mean normalization can degrade the expressiveness of the neural networks, as mean statistics incorporate graph structural information. Motivated by this, [26] proposes GraphNorm, which employs a learnable shift to preserve the mean statistics to a certain extent. The study reports that GraphNorm consistently achieves superior convergence speed and training stability on graph classification for GNNs over other normalization strategies.

3.2 Bias in GNNs

ML models can lead to discriminative results towards certain under-represented groups, as they propagate the bias within the training data [10, 11]. It has been demonstrated that the utilization of graph structure in GNNs amplifies the already existing bias [12]. Thus, understanding the sources of bias in graph structure is crucial to develop a remedy for it. Motivated by this, [28] and [29] investigate the sources of bias in GNN-based learning. In [28], the representation discrepancy between different sensitive groups is examined, whereas in [29], the bias analysis is based on the correlation between the aggregated representations \mathbf{Z} and sensitive attributes \mathbf{s} . Though through

different approaches, both analyses in [28, Theorem 4.1] and [29, Theorem 3.1] demonstrate the parallelism between the terms $\|\boldsymbol{\mu}^{(0)} - \boldsymbol{\mu}^{(1)}\|$, $\|\boldsymbol{\Delta}\|$ and bias in GNN-based learning. Here, $\boldsymbol{\mu}^{(0)}$ and $\boldsymbol{\mu}^{(1)}$ are the sample means of node representations respectively across each sensitive group, where $\boldsymbol{\mu}^{(n)} = \text{mean}(\mathbf{h}_j \mid v_j \in \mathcal{S}^n)$, and $\boldsymbol{\Delta}$ stands for the maximal deviations of hidden representations, that is $\Delta_i^{(n)} = \max_j |h_{i,j}^{(n)} - \mu_i^{(n)}|, \forall i = 1, \dots, F$ and $\boldsymbol{\Delta} = \max(\boldsymbol{\Delta}^{(0)}, \boldsymbol{\Delta}^{(1)})$. The superscript (n) in $\mathbf{h}_j^{(n)}$ is utilized to specify the sensitive group index. Specifically, the hidden representation $\mathbf{h}_j^{(n)}$ corresponds to a node $v_j \in \mathcal{S}^n$.

As the analyses in [28, 29] suggest that the distributions of hidden representations corresponding to different sensitive groups \mathcal{S}^0 and \mathcal{S}^1 influence the resulted bias by GNNs, a tool that can shift these group-wise distributions can effectively decrease bias-related terms, and hence the overall bias.

4 FairNorm: A Fair and Fast Training Framework for GNNs

This section presents the proposed unified framework that achieves fairness improvement together with faster convergence speed for GNN-based learning.

4.1 Group-wise Normalization

It has been demonstrated in [28, 29] that decreasing $\|\boldsymbol{\mu}^{(0)} - \boldsymbol{\mu}^{(1)}\|$ and $\boldsymbol{\Delta}$ can effectively reduce bias in GNN-based learning. Note that both terms are affected by the distributions of representations from different sensitive groups. On the other hand, the mean and standard deviation of the hidden representations, and in turn their distributions, are affected by the learnable parameters of a normalization layer. Thus, employing such a layer can enable manipulating said distributions, which can be used to improve fairness. Inspired by this, the proposed framework, FairNorm, first applies normalizations to different sensitive groups individually, which results in individual learnable parameters affecting $\boldsymbol{\mu}^{(0)}$, and $\boldsymbol{\mu}^{(1)}$, as well as their difference. For any input matrix $\mathbf{A} \in \mathbb{R}^{F \times N}$, given that the columns of \mathbf{A} can be divided into two sensitive groups \mathcal{S}^0 and \mathcal{S}^1 , the corresponding multiple group-wise normalization operations can be mathematically described as:

$$\text{M-Norm} \left(a_{i,j}^{(n)} \right) = \gamma_i^{(n)} \cdot \frac{a_{i,j}^{(n)} - \alpha_i^{(n)} \cdot m_i^{(n)}}{\sigma_i^{(n)}} + \beta_i^{(n)}, \forall i = 1, \dots, F \text{ and } n = 0, 1 \quad (1)$$

where $m_i^{(n)} = \frac{\sum_{j=1}^{|\mathcal{S}^n|} a_{i,j}^{(n)}}{|\mathcal{S}^n|}$, $(\sigma_i^{(n)})^2 = \frac{\sum_{j=1}^{|\mathcal{S}^n|} (a_{i,j}^{(n)} - m_i^{(n)})^2}{|\mathcal{S}^n|}$, and $\alpha_i^{(n)}, \gamma_i^{(n)}, \beta_i^{(n)}$ are learnable parameters. The superscript (n) in $\mathbf{a}_j^{(n)}$ specifies that the representation corresponds to a node from the sensitive group \mathcal{S}^n . Considering that mean normalization can degrade the expressiveness of GNNs [26], the proposed framework employs the learnable parameter α that manages the amount of mean normalization.

It is demonstrated in [26] that applying a shift operation over the whole graph can speed up the convergence for graph classification. However, as the proposed framework herein applies multiple shift operations individually over subgraphs corresponding to different sensitive groups and considers the node classification task, the effect of the proposed strategy on the convergence speed becomes unclear. Hence, the analysis in [26] cannot be directly applied to this case. Motivated by this, this study analytically examines the influence of group-wise shifts on the convergence speed.

Shift operations over different sensitive groups can be applied in matrix forms via the matrices $\mathbf{N}^{(0)}$ and $\mathbf{N}^{(1)}$, where $\mathbf{N}^{(n)} = \mathbf{I}_N - \frac{1}{|\mathcal{S}^n|} \mathbf{e}^{(n)} (\mathbf{e}^{(n)})^\top$ for $n = 0, 1$. In this formulation, $\mathbf{e}^{(n)} \in \mathbb{R}^N$ is created such that $e_j^{(n)} = 1$ if $v_j \in \mathcal{S}^n$, and $e_j^{(n)} = 0$ otherwise. Therefore, for any vector $\mathbf{c} \in \mathbb{R}^N$, $\mathbf{c}^\top \mathbf{N}^{(n)} = \mathbf{c}^\top - \left(\frac{1}{|\mathcal{S}^n|} \sum_{j: v_j \in \mathcal{S}^n} c_j \right) (\mathbf{e}^{(n)})^\top$. Hence, the group-wise shift operations applied to hidden representations can be written as:

$$\text{MShift}(\mathbf{W}^{(k)} \mathbf{H}^{(k-1)} \mathbf{Q}) = \mathbf{W}^{(k)} \mathbf{H}^{(k-1)} \mathbf{Q} \mathbf{N}^{(0)} \mathbf{N}^{(1)}. \quad (2)$$

The following lemma demonstrates that $\mathbf{N}^{(0)} \mathbf{N}^{(1)}$ acts as a preconditioner of \mathbf{Q} , whose proof is presented in Appendix A.

Lemma 1. Let $0 \leq \lambda_1 \leq \dots \leq \lambda_N$ be the singular values of \mathbf{Q} . We have $\gamma_N = \gamma_{N-1} = 0$ as the two of the singular values of $\mathbf{Q}\mathbf{N}^0\mathbf{N}^1$. Let the remaining singular values of $\mathbf{Q}\mathbf{N}^0\mathbf{N}^1$ be $0 \leq \gamma_1 \leq \gamma_2 \leq \dots \leq \gamma_{N-2}$. Then, the following holds:

$$\begin{aligned} \lambda_1 &\leq \gamma_1 \\ \lambda_2 &\leq \gamma_2 \\ &\vdots \\ \lambda_{N-2} &\leq \gamma_{N-2} \leq \lambda_N, \end{aligned} \quad (3)$$

where $\lambda_i = \gamma_i$ or $\lambda_N = \gamma_{N-2}$, only if \mathbf{Q} have a right singular vector $\boldsymbol{\alpha}$ such that $(\mathbf{e}^{(0)})^\top \boldsymbol{\alpha} = 0$ and $(\mathbf{e}^{(1)})^\top \boldsymbol{\alpha} = 0$.

In other domains, such as DNNs or iterative algorithms, a similar preconditioning is considered to help the training [45, 46]. Such a preconditioning of the aggregation matrix \mathbf{Q} is also demonstrated to accelerate the optimization of GNNs [26]. In order to theoretically investigate such an effect in our setting, we considered a basic linear GNN model for node classification that is optimized via gradient descent, and presented its convergence analysis in Theorem 1. Appendix B presents all assumptions and considered learning settings employed in Theorem 1 in detail, as well as its proof.

Theorem 1. For a linear GNN model, let the parameters of the model at time t with applied shift operations through $\mathbf{N}^0\mathbf{N}^1$ be denoted by \mathbf{w}_t^{MShift} . Then, with high probability, \mathbf{w}_t^{MShift} converges to the optimal parameters \mathbf{w}_*^{MShift} linearly with a rate ρ_1 :

$$\left\| \mathbf{w}_t^{MShift} - \mathbf{w}_*^{MShift} \right\|_2 = O(\rho_1^t). \quad (4)$$

The same also holds for the parameters of the model without any shift, $\mathbf{w}^{vanilla}$, for convergence rate ρ_2 :

$$\left\| \mathbf{w}_t^{Vanilla} - \mathbf{w}_*^{Vanilla} \right\|_2 = O(\rho_2^t), \quad \text{where } \rho_1 < \rho_2. \quad (5)$$

Thus, it concludes that the shift operations applied through $\mathbf{N}^0\mathbf{N}^1$ lead to faster convergence with high probability compared to the scheme where no shift is applied.

Theorem 1 demonstrates that the individual shift operations applied over different sensitive groups indeed improve the convergence rate compared to the naive baseline. While the result of Theorem 1 seems to be similar to the result of [26, Proposition 3.1], the analysis in [26] cannot be easily extended to our proof due to the employment of group-wise shifts in this work and the fact that we consider node classification instead of graph classification.

4.2 Fairness-aware Regularizers

Consider the conventional case where the normalization is applied after linear transformations [13, 17, 26]. For this case, the hidden representations can be expressed in matrix form as:

$$\mathbf{H}^{(n)} = \text{Act} \left(\text{M-Norm}^{(n)} \left((\mathbf{WHQ})^{(n)} \right) \right), \quad \text{for } n = 0, 1. \quad (6)$$

In Equation (6), $(\mathbf{WHQ})^{(n)}$ denotes the submatrix consisting the columns of (\mathbf{WHQ}) whose corresponding nodes are in \mathcal{S}^n . Furthermore, as the proposed strategy applies normalizations individually over different sensitive groups, these group-wise normalization layers are differentiated by the superscript $n = 0, 1$. Let $\bar{\boldsymbol{\mu}}^{(n)} \in \mathbb{R}^F$ denote the sample mean of representations after normalization for the sensitive group \mathcal{S}^n , $n = 0, 1$. In the proposed framework, recalling from Subsection 4.1, individual normalization layers are employed to create individual learnable parameters for the distributions of different sensitive groups, so that the bias-related terms derived in [28, 29] can be reduced. However, in order to manipulate $\bar{\boldsymbol{\mu}}^{(0)}$ and $\bar{\boldsymbol{\mu}}^{(1)}$ for possible bias reduction, the relationship between $\|\boldsymbol{\mu}^{(0)} - \boldsymbol{\mu}^{(1)}\|$ and $\bar{\boldsymbol{\mu}}^{(n)}$'s should be investigated. To this end, we present the following theorem, the proof of which can be found in Appendix C.

Theorem 2. Let $\text{Act}(\cdot)$ be Lipschitz continuous with Lipschitz constant L , and let $\bar{\mathbf{H}}^{(n)}$ denote the normalized representations in group \mathcal{S}^n . Then, $\|\boldsymbol{\mu}^{(0)} - \boldsymbol{\mu}^{(1)}\|$ is bounded above by

$$\|\boldsymbol{\mu}^{(0)} - \boldsymbol{\mu}^{(1)}\|_p \leq L \left(\|\bar{\boldsymbol{\mu}}^{(0)} - \bar{\boldsymbol{\mu}}^{(1)}\|_p + \|\bar{\boldsymbol{\Delta}}^{(0)}\|_p + \|\bar{\boldsymbol{\Delta}}^{(1)}\|_p \right), \quad \forall p \geq 1. \quad (7)$$

Here, $\bar{\Delta}^{(n)}$ is the maximal deviation of $\bar{\mathbf{H}}^{(n)}$ from $\bar{\boldsymbol{\mu}}^{(n)}$ (i.e., we have $\bar{\Delta}_i^{(n)} = \max_j |\bar{h}_{i,j}^{(n)} - \bar{\mu}_i^{(n)}|, \forall i = 1, \dots, F$).

Theorem 2 demonstrates that decreasing $\|\bar{\boldsymbol{\mu}}^{(0)} - \bar{\boldsymbol{\mu}}^{(1)}\|$ results in a decreased upper bound for $\|\boldsymbol{\mu}^{(0)} - \boldsymbol{\mu}^{(1)}\|$, which can possibly reduce the actual value of $\|\boldsymbol{\mu}^{(0)} - \boldsymbol{\mu}^{(1)}\|$. Based on this result, as a second step after applying individual normalization layers over different sensitive groups, FairNorm proposes the use of a regularizer term $\mathcal{L}_\mu = \|\bar{\boldsymbol{\mu}}^{(0)} - \bar{\boldsymbol{\mu}}^{(1)}\|_2^2$ to decrease bias for GNN-based learning. We note that many commonly used activation functions such as ReLU, sigmoid, tanh, *etc.* have a Lipschitz constant equal to $L = 1$.

Furthermore, Theorem 2 shows that the upper bound for $\|\boldsymbol{\mu}^{(0)} - \boldsymbol{\mu}^{(1)}\|$ can also be decreased by reducing the norms of maximal deviations $\bar{\Delta}^{(0)}$ and $\bar{\Delta}^{(1)}$. Inspired by this finding, $\mathcal{L}_\Delta = \|\bar{\Delta}^{(0)}\|_2^2 + \|\bar{\Delta}^{(1)}\|_2^2$ is also introduced as a regularizer to reduce the norms of maximal deviations of the normalized representations. Hence, the overall learning objective for the considered node classification task can be written as:

$$\min_{\theta_{GNN}} \mathcal{L}_c + \kappa \mathcal{L}_\mu + \tau \mathcal{L}_\Delta \quad (8)$$

where \mathcal{L}_c is the classification loss, $\mathcal{L}_\mu = \|\bar{\boldsymbol{\mu}}^{(0)} - \bar{\boldsymbol{\mu}}^{(1)}\|_2^2 = \left\| \left(\gamma^{(0)} \frac{\mathbf{m}^{(0)}(1-\alpha^{(0)})}{\sigma^{(0)}} + \beta^{(0)} \right) - \left(\gamma^{(1)} \frac{\mathbf{m}^{(1)}(1-\alpha^{(1)})}{\sigma^{(1)}} + \beta^{(1)} \right) \right\|_2^2$ for M-Norm in (1). $\mathcal{L}_\Delta = \|\bar{\Delta}^{(0)}\|_2^2 + \|\bar{\Delta}^{(1)}\|_2^2$, and $\bar{\Delta}_i^{(n)} = \frac{\gamma_i^{(n)}}{\sigma_i^{(n)}} \max_j |r_{i,j}^{(n)} - m_i^{(n)}|$ for M-Norm defined in (1) $\forall i = 1, \dots, F$, where $\mathbf{R}^{(n)} = (\mathbf{W}\mathbf{H}\mathbf{Q})^{(n)}$ denotes the representations input to the normalization layer. GNN parameters are denoted by θ_{GNN} , and κ and τ are hyperparameters specifying the focus on the fairness regularizers.

Remark 1 (Order of normalization and activation). Although the proposed fairness regularizers $\mathcal{L}_\mu, \mathcal{L}_\Delta$ are designed for the conventional case where the normalization is used before nonlinear activation, it can be demonstrated that they can also reduce bias when the normalization is applied after activation, where

$$\mathbf{H}^{(n)} = \text{M-Norm}^{(n)} \left(\text{Act} \left((\mathbf{W}\mathbf{H}\mathbf{Q})^{(n)} \right) \right), \text{ for } n = 0, 1. \quad (9)$$

In this case, it holds that $\bar{\boldsymbol{\mu}}^{(n)} = \boldsymbol{\mu}^{(n)}$ and $\|\bar{\Delta}^{(n)}\| = \|\Delta^{(n)}\|$ for $n = 0, 1$. Therefore, the employment of the proposed fairness regularizers can naturally be extended to the case where the normalization is utilized after activation, as the analyses in [28, 29] demonstrate that reducing $\|\boldsymbol{\mu}^{(0)} - \boldsymbol{\mu}^{(1)}\|$ and $\|\Delta\|$ can help mitigate bias in GNN-based learning.

Remark 2 (Non-binary sensitive attributes). It is worth mentioning that, while the fairness analyses in [28, 29] are carried out only for a single and binary sensitive attribute, the proposed framework can be extended to non-binary sensitive attributes as well. For non-binary attributes, the normalization layers can still be applied independently for each sensitive group. Afterwards, via regularizers, the sample means for different groups can be brought closer based on distance measures of choice (e.g., the maximum of the ℓ_2 -norm distances between all pairs), as well as the norms of the maximal deviations of normalized representations corresponding to different sensitive groups can be decreased.

Remark 3 (Applicability to other normalization methods). Note that the proposed FairNorm framework can be readily utilized together with other normalization techniques where the distribution of the normalized representations depends on learnable parameters, e.g., BatchNorm [13].

5 Experiments

In this section, experimental results obtained on real-world datasets for a supervised node classification task are presented. The performance of the proposed framework, FairNorm, is compared with baseline schemes in terms of node classification accuracy and fairness metrics. Furthermore, the influence of the proposed fairness-aware normalization strategy on convergence speed is examined.

5.1 Datasets and Settings

Datasets. In the experiments, three real-world networks are used: Pokec-z, Pokec-n [12], and the Recidivism graph [47]. Pokec-z and Pokec-n are created by sampling the anonymized, 2012 version of Pokec [48], which is a Facebook-like social network used in Slovakia [12]. In Pokec networks, the region information is utilized as the sensitive attribute, where the nodes of these graphs are the users living in two major regions. Labels to be used in node classification are assigned to be the binarized working field of the users. The information of defendants (corresponding to nodes) who got released on bail at the U.S. state courts during 1990-2009 [47] is utilized to build the Recidivism graph, where the edges are formed based on the similarity of past criminal records and demographics. Race is used as the sensitive attribute for this graph, and the node classification task classifies defendants into bail (i.e., the defendant is not likely to commit a violent crime if released) or no bail (i.e., the defendant is likely to commit a violent crime if released) [39]. Further statistical information for datasets are presented in Table 2 in Appendix D.

Evaluation Metrics. Accuracy is used as the utility measure for node classification. Two quantitative measures of group fairness metrics are also reported in terms of **statistical parity**: $\Delta_{SP} = |P(\hat{y} = 1 | s = 0) - P(\hat{y} = 1 | s = 1)|$ and **equal opportunity**: $\Delta_{EO} = |P(\hat{y} = 1 | y = 1, s = 0) - P(\hat{y} = 1 | y = 1, s = 1)|$, where y is the ground truth label, and \hat{y} denotes the predicted label. Lower values for Δ_{SP} and Δ_{EO} signify better fairness performance [12].

Implementation details. To comparatively evaluate our proposed framework, node classification is utilized in a supervised setting. A two-layer GCN [4] followed by a linear layer is employed for the classification task, which is identical to the experimental setting used in [12]. A normalization layer follows after every GNN layer, where the normalization is applied after linear transformations and before the non-linear activation, as suggested in [13, 26]. For the hyperparameter selection of the GCN model, See Appendix E. This experimental framework is kept the same for all baselines. Furthermore, training of the model is executed over 50% of the nodes, while the remaining nodes are equally divided to be used as the validation and test sets. For each experiment, results for five random data splits are obtained, and the average of them together with standard deviations are presented. The hyperparameters of the proposed fairness-aware framework and all other baselines are tuned via a grid search on cross-validation sets, see Appendix E for the utilized hyperparameter values. A sensitivity analysis is also provided in Appendix F for the hyperparameters of the proposed FairNorm framework.

Baselines. This work aims to mitigate bias via employing fairness-aware regularizers, as well as to provide a faster convergence through its utilized normalization layers. We note that similar to the proposed regularizers, any other fairness-aware regularizer can be employed together with a normalization layer, for these same purposes. In order to demonstrate the performance improvement of the proposed regularizers over said alternatives, we compare the proposed framework with other fairness-aware regularizers. To this end, the performance of 4 different baselines is presented. For improving fairness in a supervised setting, FairGNN [12] employs adversarial debiasing and a covariance-based regularizer (the absolute covariance between the sensitive attribute and estimated label \hat{y}). The results for these regularizers are obtained both individually and together, where the framework that utilizes both regularizers is called FairGNN [12]. Furthermore, hyperbolic tangent relaxation of the difference of demographic parity (HTR_{DDP}) that is proposed in [49] is utilized as another baseline. Note that, as DDP is not differentiable, its relaxations are used as fairness-aware regularizers for a gradient-based optimization. It is worth emphasizing that the fairness regularizers proposed in this study are also applicable to an unsupervised setting, while the covariance-based (also FairGNN) and HTR_{DDP} regularizers can only be used in a supervised framework.

5.2 Experimental Results

The results of node classification are presented in Table 1 in terms of fairness and utility metrics for both the proposed framework and baselines. The results are obtained for two commonly utilized activation functions: ReLU and sigmoid, in order to demonstrate the efficacy of the proposed framework over different activations. In Table 1, “NoNorm” denotes the scheme where no normalization layer is employed. “M-Norm” stands for the proposed framework where only individual normalizations are applied to the nodes belonging to different sensitive groups, without using the proposed fairness regularizers. Furthermore, “Covariance” is for the covariance-based regularizer [12], “Adversarial” stands for the adversarial regularizer [12], and “ HTR_{DDP} ” denotes hyperbolic tangent relaxation

Table 1: Comparative Results with Baselines for Different Activation Function Selections

ReLU	Pokec-z			Pokec-n			Recidivism		
	Acc (%)	Δ_{SP} (%)	Δ_{EO} (%)	Acc (%)	Δ_{SP} (%)	Δ_{EO} (%)	Acc (%)	Δ_{SP} (%)	Δ_{EO} (%)
NoNorm	70.24 ± 1.0	6.77 ± 1.8	6.18 ± 2.5	69.29 ± 0.8	1.66 ± 1.6	2.19 ± 1.8	94.32 ± 0.2	8.89 ± 0.7	1.17 ± 0.9
M-Norm	70.71 ± 0.8	5.57 ± 1.3	5.00 ± 2.0	69.25 ± 0.5	2.48 ± 1.2	2.91 ± 1.7	95.00 ± 0.3	8.87 ± 1.2	1.71 ± 0.7
Covariance	70.66 ± 0.8	5.31 ± 1.4	4.56 ± 1.9	69.47 ± 0.6	2.06 ± 1.3	2.42 ± 1.5	95.07 ± 0.2	8.82 ± 1.1	1.43 ± 0.6
Adversarial	70.35 ± 0.9	2.41 ± 1.0	2.16 ± 0.6	69.30 ± 0.4	2.09 ± 1.9	2.21 ± 1.9	94.14 ± 0.1	8.58 ± 1.0	1.26 ± 0.7
FairGNN	70.34 ± 1.1	2.78 ± 1.5	2.73 ± 1.0	69.21 ± 0.4	2.03 ± 1.9	2.29 ± 2.1	95.14 ± 0.2	8.73 ± 1.0	1.33 ± 0.8
<i>HTR_{DDP}</i>	70.38 ± 0.9	2.12 ± 2.0	3.38 ± 1.5	69.51 ± 0.5	1.85 ± 1.4	2.03 ± 1.5	95.16 ± 0.2	8.74 ± 0.8	1.05 ± 0.4
FairNorm	70.67 ± 1.0	1.35 ± 1.2	1.90 ± 1.8	69.38 ± 0.7	1.26 ± 1.2	1.22 ± 1.3	95.11 ± 0.2	8.45 ± 1.0	0.90 ± 0.5

Sigmoid	Pokec-z			Pokec-n			Recidivism		
	Acc (%)	Δ_{SP} (%)	Δ_{EO} (%)	Acc (%)	Δ_{SP} (%)	Δ_{EO} (%)	Acc (%)	Δ_{SP} (%)	Δ_{EO} (%)
NoNorm	70.25 ± 0.8	7.40 ± 1.8	6.04 ± 3.1	68.73 ± 0.6	2.68 ± 2.2	2.27 ± 2.4	92.69 ± 0.2	8.29 ± 0.7	1.31 ± 0.6
M-Norm	69.84 ± 0.7	6.21 ± 1.4	4.44 ± 2.1	68.59 ± 0.9	1.78 ± 2.1	2.88 ± 1.8	94.45 ± 0.3	8.94 ± 1.2	2.06 ± 1.0
Covariance	69.77 ± 0.6	5.63 ± 1.9	4.04 ± 2.1	68.40 ± 1.1	1.70 ± 2.2	2.26 ± 1.8	92.87 ± 1.0	8.44 ± 0.6	1.64 ± 1.0
Adversarial	70.01 ± 0.9	3.08 ± 2.8	3.00 ± 2.4	68.47 ± 0.7	1.56 ± 1.8	2.25 ± 1.5	93.82 ± 0.2	8.72 ± 0.9	1.59 ± 1.1
FairGNN	69.93 ± 0.7	4.55 ± 2.2	4.71 ± 2.7	68.42 ± 0.7	1.61 ± 1.7	1.71 ± 2.0	94.11 ± 0.2	8.68 ± 1.2	1.51 ± 0.5
<i>HTR_{DDP}</i>	69.74 ± 0.7	1.85 ± 1.1	2.27 ± 1.8	68.37 ± 0.9	1.64 ± 1.6	2.53 ± 1.7	93.34 ± 0.4	8.20 ± 0.9	1.04 ± 1.0
FairNorm	69.73 ± 0.9	1.71 ± 0.3	1.48 ± 1.1	68.88 ± 1.1	1.44 ± 1.2	1.74 ± 1.7	94.32 ± 0.2	7.28 ± 1.1	0.80 ± 0.9

of the difference of demographic parity [49]. It should be noted that the results for baselines are obtained with the best performing normalization layer framework (individual normalizations over different sensitive groups vs. normalization over all nodes in the graph) in terms of fairness measures.

The results in Table 1 demonstrate that FairNorm achieves superior fairness performance, together with similar utility, compared to all baselines on all datasets, for both of the utilized activation functions. Compared to its natural baseline “M-Norm”, FairNorm achieves approximately 70% improvement in all fairness measures on Pokec-z. Furthermore, on the Recidivism graph with sigmoid activation, while the improvement in fairness metrics is accompanied by a decrease in accuracy for the baselines, FairNorm achieves better fairness performance without a deterioration in utility. Overall, the results in Table 1 show the efficacy of the proposed fairness regularizers in reducing bias while providing similar utility on different real-world networks. Note that, in addition to their superior fairness performance, the proposed regularizers of FairNorm can be flexibly applied to both supervised and unsupervised settings, whereas some of the baselines (“Covariance”, “FairGNN”, “*HTR_{DDP}*”) require predicted labels for their regularizer designs.

Remark 4 (Ablation study). An ablation study is also provided in Appendix G in order to demonstrate the influences of \mathcal{L}_μ and \mathcal{L}_Δ independently. Overall, the ablation study signifies that while \mathcal{L}_μ has a greater effect on fairness improvement compared to \mathcal{L}_Δ , the utilization of both regularizers typically leads to the largest improvement in fairness measures.

The proposed framework herein aims to mitigate bias by also providing a faster convergence speed. The results in Table 1 confirm that the proposed fairness regularizers within FairNorm do provide said bias reduction. In order to evaluate the convergence speed of FairNorm’s group-wise normalizations, Figure 1 is presented. The baselines in Figure 1 consist of GraphNorm [26], and the framework where no normalization is applied. We note that in Figure 1, Fairnorm is employed with both its individual normalizations as well as its fairness regularizers.

The results on both Pokec datasets and the Recidivism network confirm that the employed normalization can indeed lead to a faster convergence in training compared to NoNorm. Figure 1 also demonstrates that compared to GraphNorm, the convergence improvement of FairNorm is slightly less on Pokec-z, whereas it provides approximately the same improvement on Pokec-n and Recidivism.

6 Conclusions and Limitations

This study proposes a unified framework, FairNorm, that mitigates bias in GNN-based learning and provides faster convergence in training. FairNorm applies normalization independently over different sensitive groups, and employs two novel fairness regularizers that manipulate the parameters of these normalization layers. The designs of these regularizers are based on theoretical fairness analyses on GNNs. Experimental results on real-world social networks show the fairness improvement of FairNorm over fairness-aware baselines in terms of statistical parity and equal opportunity, as well

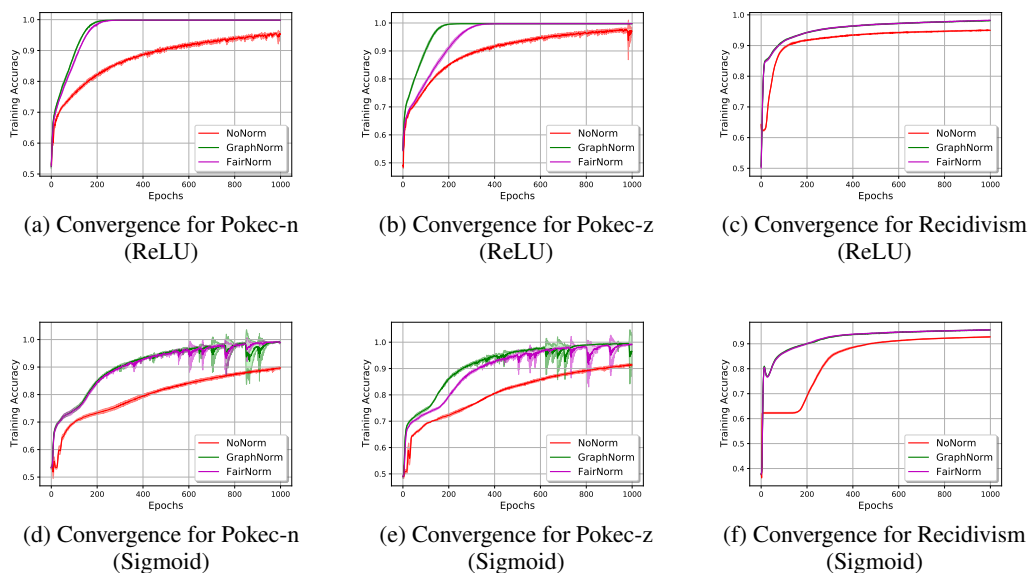


Figure 1: Convergence for different graph data sets when the normalization is not applied (Nonorm) and applied with/without fairness consideration (FairNorm/GraphNorm).

as its similar utility performance in node classification tasks. Furthermore, it is demonstrated that FairNorm improves the convergence speed of the naive baseline where no normalization is used.

The present framework considers only a single sensitive attribute in its design of normalization layers and fairness regularizers. One possible future direction of this study is the extension of the current design to a case with multiple sensitive attributes, which may be essential in certain applications. Furthermore, while the experimental results are obtained in a supervised setting for fair comparison with certain baselines, FairNorm is also applicable to an unsupervised setting. Thus, another future direction is to investigate the performance of FairNorm in an unsupervised learning setting.

References

- [1] M. Gori, G. Monfardini, and F. Scarselli, “A new model for learning in graph domains,” in *Proc. IEEE International Joint Conference on Neural Networks (IJCNN)*, vol. 2, no. 2005, 2005, pp. 729–734.
- [2] F. Scarselli, M. Gori, A. C. Tsoi, M. Hagenbuchner, and G. Monfardini, “The graph neural network model,” *IEEE Transactions on Neural Networks*, vol. 20, no. 1, pp. 61–80, 2008.
- [3] W. Hamilton, Z. Ying, and J. Leskovec, “Inductive representation learning on large graphs,” *Advances in Neural Information Processing Systems (NeurIPS)*, vol. 30, December 2017.
- [4] T. N. Kipf and M. Welling, “Semi-supervised classification with graph convolutional networks,” in *Proc. International Conference on Learning Representations (ICLR)*, April 2017.
- [5] P. Veličković, G. Cucurull, A. Casanova, A. Romero, P. Liò, and Y. Bengio, “Graph attention networks,” in *Proc. International Conference on Learning Representations (ICLR)*, April 2018.
- [6] K. Xu, C. Li, Y. Tian, T. Sonobe, K.-i. Kawarabayashi, and S. Jegelka, “Representation learning on graphs with jumping knowledge networks,” in *Proc. International Conference on Machine Learning (ICML)*, July 2018, pp. 5453–5462.
- [7] F. L. Opolka, A. Solomon, C. Cangea, P. Veličković, P. Liò, and R. D. Hj elm, “Spatio-temporal deep graph infomax,” *arXiv preprint arXiv:1904.06316*, April 2019.
- [8] G. Jin, Q. Wang, C. Zhu, Y. Feng, J. Huang, and J. Zhou, “Addressing crime situation forecasting task with temporal graph convolutional neural network approach,” in *Proc. International Conference on Measuring Technology and Mechatronics Automation (ICMTMA)*, February 2020, pp. 474–478.

- [9] R. Ying, R. He, K. Chen, P. Eksombatchai, W. L. Hamilton, and J. Leskovec, “Graph convolutional neural networks for web-scale recommender systems,” in *Proc. ACM International Conference on Knowledge Discovery & Data Mining (SIGKDD)*, July 2018, pp. 974–983.
- [10] C. Dwork, M. Hardt, T. Pitassi, O. Reingold, and R. Zemel, “Fairness through awareness,” in *Proc. Innovations in Theoretical Computer Science (ITCS)*, January 2012, pp. 214–226.
- [11] A. Beutel, J. Chen, Z. Zhao, and E. H. Chi, “Data decisions and theoretical implications when adversarially learning fair representations,” *arXiv preprint arXiv:1707.00075*, June 2017.
- [12] E. Dai and S. Wang, “Say no to the discrimination: Learning fair graph neural networks with limited sensitive attribute information,” in *Proc. 14th ACM International Conference on Web Search and Data Mining (WSDM)*, March 2021, pp. 680–688.
- [13] S. Ioffe and C. Szegedy, “Batch normalization: Accelerating deep network training by reducing internal covariate shift,” in *Proc. International Conference on Machine Learning (ICML)*, July 2015, pp. 448–456.
- [14] D. Ulyanov, A. Vedaldi, and V. Lempitsky, “Instance normalization: The missing ingredient for fast stylization,” *arXiv preprint arXiv:1607.08022*, 2016.
- [15] J. L. Ba, J. R. Kiros, and G. E. Hinton, “Layer normalization,” *arXiv preprint arXiv:1607.06450*, 2016.
- [16] T. Salimans and D. P. Kingma, “Weight normalization: A simple reparameterization to accelerate training of deep neural networks,” *Advances in Neural Information Processing Systems (NeurIPS)*, vol. 29, December 2016.
- [17] R. Xiong, Y. Yang, D. He, K. Zheng, S. Zheng, C. Xing, H. Zhang, Y. Lan, L. Wang, and T. Liu, “On layer normalization in the transformer architecture,” in *Proc. International Conference on Machine Learning (ICML)*, July 2020, pp. 10 524–10 533.
- [18] T. Miyato, T. Kataoka, M. Koyama, and Y. Yoshida, “Spectral normalization for generative adversarial networks,” in *Proc. International Conference on Learning Representations (ICLR)*, April 2018.
- [19] Y. Wu and K. He, “Group normalization,” in *Proc. European conference on computer vision (ECCV)*, October 2018, pp. 3–19.
- [20] S. Santurkar, D. Tsipras, A. Ilyas, and A. Madry, “How does batch normalization help optimization?” *Advances in Neural Information Processing Systems (NeurIPS)*, vol. 31, December 2018.
- [21] F. Scarselli, A. C. Tsoi, and M. Hagenbuchner, “The vapnik–chervonenkis dimension of graph and recursive neural networks,” *Neural Networks*, vol. 108, pp. 248–259, 2018.
- [22] K. Xu, J. Li, M. Zhang, S. S. Du, K.-i. Kawarabayashi, and S. Jegelka, “What can neural networks reason about?” in *Proc. International Conference on Learning Representations (ICLR)*, April 2019.
- [23] K. Xu, W. Hu, J. Leskovec, and S. Jegelka, “How powerful are graph neural networks?” in *Proc. International Conference on Learning Representations (ICLR)*, April 2018.
- [24] A. Loukas, “How hard is to distinguish graphs with graph neural networks?” *Advances in Neural Information Processing Systems (NeurIPS)*, vol. 33, pp. 3465–3476, December 2020.
- [25] C. Ying, T. Cai, S. Luo, S. Zheng, G. Ke, D. He, Y. Shen, and T.-Y. Liu, “Do transformers really perform badly for graph representation?” *Advances in Neural Information Processing Systems (NeurIPS)*, vol. 34, December 2021.
- [26] T. Cai, S. Luo, K. Xu, D. He, T.-y. Liu, and L. Wang, “Graphnorm: A principled approach to accelerating graph neural network training,” in *Proc. International Conference on Machine Learning (ICML)*, July 2021, pp. 1204–1215.
- [27] M. Balunovic, A. Ruoss, and M. Vechev, “Fair normalizing flows,” in *Proc. International Conference on Learning Representations (ICLR)*, April 2021.
- [28] P. Li, Y. Wang, H. Zhao, P. Hong, and H. Liu, “On dyadic fairness: Exploring and mitigating bias in graph connections,” in *Proc. International Conference on Learning Representations (ICLR)*, April 2020.
- [29] O. D. Kose and Y. Shen, “Fair node representation learning via adaptive data augmentation,” *arXiv preprint arXiv:2201.08549*, 2022.

- [30] T. A. Rahman, B. Surma, M. Backes, and Y. Zhang, “Fairwalk: Towards fair graph embedding,” in *Proc. International Joint Conference on Artificial Intelligence (IJCAI)*, August 2019, pp. 3289–3295.
- [31] A. Bose and W. Hamilton, “Compositional fairness constraints for graph embeddings,” in *Proc. International Conference on Machine Learning (ICML)*, July 2019, pp. 715–724.
- [32] J. Fisher, A. Mittal, D. Palfrey, and C. Christodoulopoulos, “Debiasing knowledge graph embeddings,” in *Proc. Conference on Empirical Methods in Natural Language Processing (EMNLP)*, 2020, pp. 7332–7345.
- [33] M. Buyl and T. De Bie, “Debayes: a bayesian method for debiasing network embeddings,” in *Proc. International Conference on Machine Learning (ICML)*, July 2020, pp. 1220–1229.
- [34] J. Ma, J. Deng, and Q. Mei, “Subgroup generalization and fairness of graph neural networks,” *arXiv preprint arXiv:2106.15535*, 2021.
- [35] Z. Zeng, R. Islam, K. N. Keya, J. Foulds, Y. Song, and S. Pan, “Fair representation learning for heterogeneous information networks,” *arXiv preprint arXiv:2104.08769*, 2021.
- [36] M. Buyl and T. De Bie, “The kl-divergence between a graph model and its fair i-projection as a fairness regularizer,” *arXiv preprint arXiv:2103.01846*, 2021.
- [37] C. Laclau, I. Redko, M. Choudhary, and C. Largeron, “All of the fairness for edge prediction with optimal transport,” in *Proc. International Conference on Artificial Intelligence and Statistics (AISTATS)*, April 2021, pp. 1774–1782.
- [38] Y. Dong, J. Kang, H. Tong, and J. Li, “Individual fairness for graph neural networks: A ranking based approach,” in *Proc. ACM Conference on Knowledge Discovery & Data Mining (SIGKDD)*, July 2021, pp. 300–310.
- [39] C. Agarwal, H. Lakkaraju, and M. Zitnik, “Towards a unified framework for fair and stable graph representation learning,” in *Uncertainty in Artificial Intelligence (UAI)*, August 2021, pp. 2114–2124.
- [40] I. Spinelli, S. Scardapane, A. Hussain, and A. Uncini, “Fairdrop: Biased edge dropout for enhancing fairness in graph representation learning,” *IEEE Transactions on Artificial Intelligence*, 2021.
- [41] Ö. D. Köse and Y. Shen, “Fairness-aware node representation learning,” *arXiv preprint arXiv:2106.05391*, 2021.
- [42] K. M. Yi, E. Trulls, Y. Ono, V. Lepetit, M. Salzmann, and P. Fua, “Learning to find good correspondences,” in *Proc. IEEE Conference on Computer Vision and Pattern Recognition (CVPR)*, June 2018, pp. 2666–2674.
- [43] W. Sun, W. Jiang, E. Trulls, A. Tagliasacchi, and K. M. Yi, “Acne: Attentive context normalization for robust permutation-equivariant learning,” in *Proc. IEEE/CVF Conference on Computer Vision and Pattern Recognition (CVPR)*, June 2020, pp. 11 286–11 295.
- [44] V. P. Dwivedi, C. K. Joshi, T. Laurent, Y. Bengio, and X. Bresson, “Benchmarking graph neural networks,” *arXiv preprint arXiv:2003.00982*, 2020.
- [45] D. P. Kingma and J. Ba, “Adam: A method for stochastic optimization,” *arXiv preprint arXiv:1412.6980*, 2014.
- [46] O. Axelsson, “A survey of preconditioned iterative methods for linear systems of algebraic equations,” *BIT Numerical Mathematics*, vol. 25, no. 1, pp. 165–187, 1985.
- [47] K. L. Jordan and T. L. Freiburger, “The effect of race/ethnicity on sentencing: Examining sentence type, jail length, and prison length,” *Journal of Ethnicity in Criminal Justice*, vol. 13, no. 3, pp. 179–196, 2015.
- [48] L. Takac and M. Zabolovsky, “Data analysis in public social networks,” in *International Scientific Conference and International Workshop. 'Present Day Trends of Innovations'*, vol. 1, no. 6, May 2012.
- [49] K. Padh, D. Antognini, E. Lejal-Glaude, B. Faltings, and C. Musat, “Addressing fairness in classification with a model-agnostic multi-objective algorithm,” in *Uncertainty in Artificial Intelligence (UAI)*, August 2021, pp. 600–609.
- [50] R. A. Horn and C. R. Johnson, *Matrix analysis*. Cambridge university press, 2012.

- [51] W. Cui, X. Zhang, and Y. Liu, "Covariance matrix estimation from linearly-correlated gaussian samples," *IEEE Transactions on Signal Processing*, vol. 67, no. 8, pp. 2187–2195, 2019.
- [52] X. Glorot and Y. Bengio, "Understanding the difficulty of training deep feedforward neural networks," in *Proc. International Conference on Artificial Intelligence and Statistics (AISTATS)*, May 2010, pp. 249–256.
- [53] A. Paszke, S. Gross, F. Massa, A. Lerer, J. Bradbury, G. Chanan, T. Killeen, Z. Lin, N. Gimelshein, L. Antiga *et al.*, "Pytorch: An imperative style, high-performance deep learning library," in *Proc. International Conference on Neural Information Processing Systems (NeurIPS)*, vol. 32, December 2019.
- [54] A. Hagberg, P. Swart, and D. S Chult, "Exploring network structure, dynamics, and function using networkx," in *Proc. Python in Science Conference (SciPy)*, August 2008.

A Proof of Lemma 1

First, we present the following Lemma, as it will be utilized in the proof of Lemma 1.

Lemma 2. (Cauchy Interlace Theorem, [50]). Let \mathbf{A} be a Hermitian matrix of order N , and let \mathbf{B} be a principal submatrix of \mathbf{A} of order $N - 1$, such that $\mathbf{A} = \begin{pmatrix} \mathbf{B} & \mathbf{y} \\ \mathbf{y}^\top & a \end{pmatrix} \in \mathbb{R}^{N \times N}$. If $\lambda_N \leq \lambda_{N-1} \leq \dots \leq \lambda_2 \leq \lambda_1$ lists the eigenvalues of \mathbf{A} and $\gamma_N \leq \gamma_{N-1} \leq \dots \leq \gamma_3 \leq \gamma_2$ the eigenvalues of \mathbf{B} , then:

$$\lambda_N \leq \gamma_N \leq \lambda_{N-1} \leq \gamma_{N-1} \leq \dots \leq \lambda_2 \leq \gamma_2 \leq \lambda_1 \quad (10)$$

where $\lambda_i = \gamma_i$ only when there is a nonzero $\mathbf{z} \in \mathbb{R}^{N-1}$ such that $\mathbf{B}\mathbf{z} = \gamma_i\mathbf{z}$ and $\mathbf{y}^\top \mathbf{z} = 0$; if $\lambda_i = \gamma_{i-1}$ then there is a nonzero $\mathbf{z} \in \mathbb{R}^{N-1}$ such that $\mathbf{B}\mathbf{z} = \gamma_{i-1}\mathbf{z}$, $\mathbf{y}^\top \mathbf{z} = 0$.

The shift operations over different sensitive groups are defined to be:

$$\text{MShift}(\mathbf{W}^{(k)}\mathbf{H}^{(k-1)}\mathbf{Q}) = \mathbf{W}^{(k)}\mathbf{H}^{(k-1)}\mathbf{Q}\mathbf{N}^{(0)}\mathbf{N}^{(1)}, \quad (11)$$

where $\mathbf{N}^{(n)} = \mathbf{I}_N - \frac{1}{|S^n|}\mathbf{e}^{(n)}(\mathbf{e}^{(n)})^\top$ for $n = 0, 1$. Let $0 \leq \lambda_1 \leq \dots \leq \lambda_N$ be the singular values of \mathbf{Q} . Then, eigenvalues of $(\mathbf{Q})^\top \mathbf{Q}$ are $0 \leq \lambda_1^2 \leq \dots \leq \lambda_N^2$. Let γ_i^2 denote the eigenvalues of $(\mathbf{N}^{(1)})^\top (\mathbf{N}^{(0)})^\top (\mathbf{Q})^\top \mathbf{Q} \mathbf{N}^{(0)} \mathbf{N}^{(1)} = \mathbf{N}^{(1)} \mathbf{N}^{(0)} (\mathbf{Q})^\top \mathbf{Q} \mathbf{N}^{(0)} \mathbf{N}^{(1)} \forall i = 1, \dots, N$.

$(\mathbf{N}^{(0)}\mathbf{N}^{(1)})$ is a projection matrix, for which the following holds:

$$(\mathbf{N}^{(0)}\mathbf{N}^{(1)})^2 = \mathbf{N}^{(0)}\mathbf{N}^{(1)}\mathbf{N}^{(0)}\mathbf{N}^{(1)} = \mathbf{N}^{(0)}\mathbf{N}^{(0)}\mathbf{N}^{(1)}\mathbf{N}^{(1)} = \mathbf{N}^{(0)}\mathbf{N}^{(1)}, \quad (12)$$

as both $\mathbf{N}^{(0)}$ and $\mathbf{N}^{(1)}$ are symmetric projection matrices onto the orthogonal complement spaces of the subspaces spanned by $\mathbf{e}^{(0)}$ and $\mathbf{e}^{(1)}$, respectively, and $(\mathbf{N}^{(0)}\mathbf{N}^{(1)})$ commutes. Then, the following decomposition can be written: $(\mathbf{N}^{(0)}\mathbf{N}^{(1)}) = \mathbf{U} \text{diag}(1, 1, \dots, 1, 0, 0)\mathbf{U}^\top$, where $\mathbf{U} = \left[\mathbf{U}_{sub}, \frac{1}{\sqrt{|S^0|}}\mathbf{e}^{(0)}, \frac{1}{\sqrt{|S^1|}}\mathbf{e}^{(1)} \right]$. Note that $\text{diag}(\mathbf{a})$ creates a diagonal matrix $\mathbf{D} \in \mathbb{R}^{N \times N}$ with i th diagonal entry being equal to $a_i, \forall a \in \mathbb{R}^N$. This decomposition implies that the eigenvalues corresponding to the eigenvectors $\frac{1}{\sqrt{|S^0|}}\mathbf{e}^{(0)}, \frac{1}{\sqrt{|S^1|}}\mathbf{e}^{(1)}$ are zero, which can be shown as:

$$\begin{aligned} \mathbf{N}^{(0)}\mathbf{N}^{(1)}\mathbf{e}^{(0)} &= (\mathbf{I}_N - \frac{1}{|S^0|}\mathbf{e}^{(0)}(\mathbf{e}^{(0)})^\top - \frac{1}{|S^1|}\mathbf{e}^{(1)}(\mathbf{e}^{(1)})^\top + \frac{1}{|S^0|}\frac{1}{|S^1|}\mathbf{e}^{(0)}(\mathbf{e}^{(0)})^\top\mathbf{e}^{(1)}(\mathbf{e}^{(1)})^\top)\mathbf{e}^{(0)} \\ &= (\mathbf{I}_N - \frac{1}{|S^0|}\mathbf{e}^{(0)}(\mathbf{e}^{(0)})^\top - \frac{1}{|S^1|}\mathbf{e}^{(1)}(\mathbf{e}^{(1)})^\top)\mathbf{e}^{(0)}, \text{ as } \mathbf{e}^{(0)} \text{ and } \mathbf{e}^{(1)} \text{ are orthogonal,} \\ &= \mathbf{e}^{(0)} - \frac{1}{|S^0|}\mathbf{e}^{(0)}(\mathbf{e}^{(0)})^\top\mathbf{e}^{(0)} - \frac{1}{|S^1|}\mathbf{e}^{(1)}(\mathbf{e}^{(1)})^\top\mathbf{e}^{(0)} \\ &= \mathbf{e}^{(0)} - \frac{1}{|S^0|}|S^0|\mathbf{e}^{(0)}, \text{ as } (\mathbf{e}^{(0)})^\top\mathbf{e}^{(0)} = |S^0| \text{ by definition,} \\ &= \mathbf{0e}^{(0)}. \end{aligned} \quad (13)$$

The same analysis also holds for $\mathbf{e}^{(1)}$. Let γ_N^2 and γ_{N-1}^2 denote zero eigenvalues, and $0 \leq \gamma_1^2 \leq \dots \leq \gamma_{N-2}^2$ hold. Based on the decomposition of $(\mathbf{N}^{(0)}\mathbf{N}^{(1)})$, the following can be written:

$$\begin{aligned} (\mathbf{N}^{(1)})^\top (\mathbf{N}^{(0)})^\top (\mathbf{Q})^\top \mathbf{Q} \mathbf{N}^{(0)} \mathbf{N}^{(1)} &= \mathbf{N}^{(1)}\mathbf{N}^{(0)}(\mathbf{Q})^\top \mathbf{Q} \mathbf{N}^{(0)}\mathbf{N}^{(1)} \\ &= \mathbf{U} \text{diag}(1, 1, \dots, 1, 0, 0)\mathbf{U}^\top (\mathbf{Q})^\top \mathbf{Q} \mathbf{U} \text{diag}(1, 1, \dots, 1, 0, 0)\mathbf{U}^\top \\ &\sim \text{diag}(1, 1, \dots, 1, 0, 0)\mathbf{U}^\top (\mathbf{Q})^\top \mathbf{Q} \mathbf{U} \text{diag}(1, 1, \dots, 1, 0, 0), \end{aligned} \quad (14)$$

where $\mathbf{A} \sim \mathbf{B}$, if the eigenvalues of \mathbf{A} and \mathbf{B} are the same. Furthermore, denote $\text{diag}(1, 1, \dots, 1, 0, 0)$ by $\mathbf{D} \in \mathbb{R}^{N \times N}$:

$$\mathbf{D} = \begin{bmatrix} \mathbf{I}_{N-2} & [\mathbf{0}]_{N-2 \times 2} \\ [\mathbf{0}]_{2 \times N-2} & [\mathbf{0}]_{2 \times 2} \end{bmatrix}, \quad (15)$$

where $[\mathbf{0}]_{i \times j}$ denotes an all-zeros matrix with dimensions $i \times j$. Let \mathbf{C} denote $\mathbf{Q}^\top \mathbf{Q}$.

$$\begin{aligned}
& (\mathbf{N}^{(1)})^\top (\mathbf{N}^{(0)})^\top \mathbf{C} \mathbf{N}^{(0)} \mathbf{N}^{(1)} \\
& \sim \mathbf{D} \mathbf{U}^\top \mathbf{C} \mathbf{U} \mathbf{D} \\
& = \mathbf{D} \begin{bmatrix} \mathbf{U}_{sub}^\top \\ \frac{1}{\sqrt{|S^0|}} (\mathbf{e}^{(0)})^\top \\ \frac{1}{\sqrt{|S^1|}} (\mathbf{e}^{(1)})^\top \end{bmatrix} \mathbf{C} \begin{bmatrix} \mathbf{U}_{sub} & \frac{1}{\sqrt{|S^0|}} \mathbf{e}^{(0)} & \frac{1}{\sqrt{|S^1|}} \mathbf{e}^{(1)} \end{bmatrix} \mathbf{D} \\
& = \mathbf{D} \begin{bmatrix} \mathbf{U}_{sub}^\top \mathbf{C} \mathbf{U}_{sub} & \frac{1}{\sqrt{|S^0|}} \mathbf{U}_{sub}^\top \mathbf{C} \mathbf{e}^{(0)} & \frac{1}{\sqrt{|S^1|}} \mathbf{U}_{sub}^\top \mathbf{C} \mathbf{e}^{(1)} \\ \frac{1}{\sqrt{|S^0|}} (\mathbf{e}^{(0)})^\top \mathbf{C} \mathbf{U}_{sub} & \frac{1}{|S^0|} (\mathbf{e}^{(0)})^\top \mathbf{C} \mathbf{e}^{(0)} & \frac{1}{\sqrt{|S^0||S^1|}} (\mathbf{e}^{(0)})^\top \mathbf{C} \mathbf{e}^{(1)} \\ \frac{1}{\sqrt{|S^1|}} (\mathbf{e}^{(1)})^\top \mathbf{C} \mathbf{U}_{sub} & \frac{1}{\sqrt{|S^0||S^1|}} (\mathbf{e}^{(1)})^\top \mathbf{C} \mathbf{e}^{(0)} & \frac{1}{|S^1|} (\mathbf{e}^{(1)})^\top \mathbf{C} \mathbf{e}^{(1)} \end{bmatrix} \mathbf{D} \\
& = \begin{bmatrix} \mathbf{U}_{sub}^\top \mathbf{C} \mathbf{U}_{sub} & [\mathbf{0}]_{N-2 \times 2} \\ [\mathbf{0}]_{2 \times N-2} & [\mathbf{0}]_{2 \times 2} \end{bmatrix}.
\end{aligned} \tag{16}$$

As, $(\mathbf{N}^{(1)})^\top (\mathbf{N}^{(0)})^\top \mathbf{C} \mathbf{N}^{(0)} \mathbf{N}^{(1)}$ has the eigenvalues $0 \leq \gamma_1^2 \leq \dots \leq \gamma_{N-2}^2$, and $\gamma_{N-1}^2 = \gamma_N^2 = 0$, (16) shows that $\mathbf{U}_{sub}^\top \mathbf{C} \mathbf{U}_{sub} \in \mathbb{R}^{N-2 \times N-2}$ has the eigenvalues $0 \leq \gamma_1^2 \leq \dots \leq \gamma_{N-2}^2$.

Let \mathbf{R} denote $\mathbf{U}^\top \mathbf{C} \mathbf{U}$, then \mathbf{R} has the eigenvalues $0 \leq \lambda_1^2 \leq \dots \leq \lambda_N^2$, as $\mathbf{R} \sim \mathbf{C}$.

$$\mathbf{R} = \begin{bmatrix} \mathbf{U}_{sub}^\top \mathbf{C} \mathbf{U}_{sub} & \frac{1}{\sqrt{|S^0|}} \mathbf{U}_{sub}^\top \mathbf{C} \mathbf{e}^{(0)} & \frac{1}{\sqrt{|S^1|}} \mathbf{U}_{sub}^\top \mathbf{C} \mathbf{e}^{(1)} \\ \frac{1}{\sqrt{|S^0|}} (\mathbf{e}^{(0)})^\top \mathbf{C} \mathbf{U}_{sub} & \frac{1}{|S^0|} (\mathbf{e}^{(0)})^\top \mathbf{C} \mathbf{e}^{(0)} & \frac{1}{\sqrt{|S^0||S^1|}} (\mathbf{e}^{(0)})^\top \mathbf{C} \mathbf{e}^{(1)} \\ \frac{1}{\sqrt{|S^1|}} (\mathbf{e}^{(1)})^\top \mathbf{C} \mathbf{U}_{sub} & \frac{1}{\sqrt{|S^0||S^1|}} (\mathbf{e}^{(1)})^\top \mathbf{C} \mathbf{e}^{(0)} & \frac{1}{|S^1|} (\mathbf{e}^{(1)})^\top \mathbf{C} \mathbf{e}^{(1)} \end{bmatrix} \tag{17}$$

Further, define matrix $\mathbf{A} \in \mathbb{R}^{N-1 \times N-1}$ such that:

$$\mathbf{A} = \begin{bmatrix} \mathbf{U}_{sub}^\top \mathbf{C} \mathbf{U}_{sub} & \frac{1}{\sqrt{|S^0|}} \mathbf{U}_{sub}^\top \mathbf{C} \mathbf{e}^{(0)} \\ \frac{1}{\sqrt{|S^0|}} (\mathbf{e}^{(0)})^\top \mathbf{C} \mathbf{U}_{sub} & \frac{1}{|S^0|} (\mathbf{e}^{(0)})^\top \mathbf{C} \mathbf{e}^{(0)} \end{bmatrix}, \tag{18}$$

together with eigenvalues $\eta_1 \leq \dots \leq \eta_{N-1}$. Then, utilizing Lemma 2, (17) and (18), we can conclude that

$$\lambda_1^2 \leq \eta_1 \leq \lambda_2^2 \leq \eta_2 \leq \dots \leq \eta_{N-1} \leq \lambda_N^2, \tag{19}$$

where $\lambda_i^2 = \eta_i$ or $\lambda_i^2 = \eta_{i-1}$, if and only if there is a right singular vector $\boldsymbol{\alpha}$ of \mathbf{Q} such that $(\mathbf{e}^{(1)})^\top \boldsymbol{\alpha} = 0$. The proof of the condition for $\lambda_i^2 = \eta_i$ or $\lambda_i^2 = \eta_{i-1}$ is presented below in *italic*.

Proof: *Cauchy interlace theorem states that inequalities in (10) become equalities if there is a nonzero $\mathbf{z} \in \mathbb{R}^{N-1}$ such that $\mathbf{Bz} = \gamma_i \mathbf{z}$ and $\mathbf{y}^\top \mathbf{z} = 0$ or if there is a nonzero $\mathbf{z} \in \mathbb{R}^{N-1}$ such that $\mathbf{Bz} = \gamma_{i-1} \mathbf{z}$ and $\mathbf{y}^\top \mathbf{z} = 0$. Therefore, for the result in (19), inequalities become equalities, if there is a nonzero $\mathbf{z} \in \mathbb{R}^{N-1}$ such that:*

$$\mathbf{Az} = \eta \mathbf{z} \text{ and } \begin{bmatrix} \frac{1}{\sqrt{|S^1|}} (\mathbf{e}^{(1)})^\top \mathbf{C} \mathbf{U}_{sub} & \frac{1}{\sqrt{|S^0||S^1|}} (\mathbf{e}^{(1)})^\top \mathbf{C} \mathbf{e}^{(0)} \end{bmatrix} \mathbf{z} = 0. \tag{20}$$

Note that we dropped the subscript of η in (20), as it is enough to hold these conditions for any of the η_i s to turn one of the inequalities into equality in (19).

$$\mathbf{A} = \begin{bmatrix} \mathbf{U}_{sub}^\top \\ \frac{1}{\sqrt{|S^0|}} (\mathbf{e}^{(0)})^\top \end{bmatrix} \mathbf{C} \begin{bmatrix} \mathbf{U}_{sub} & \frac{1}{\sqrt{|S^0|}} \mathbf{e}^{(0)} \end{bmatrix} \tag{21}$$

Let $\mathbf{U}_1 := \begin{bmatrix} \mathbf{U}_{sub} & \frac{1}{\sqrt{|S^0|}} \mathbf{e}^{(0)} \end{bmatrix}$, where \mathbf{U}_1 forms an orthogonal basis for $\mathbf{e}^{(1)}$. Therefore, $\mathbf{A} = \mathbf{U}_1^\top \mathbf{C} \mathbf{U}_1$. The conditions presented in (20) can be rewritten based on this definition:

$$\mathbf{U}_1^\top \mathbf{C} \mathbf{U}_1 \mathbf{z} = \eta \mathbf{z} \text{ and } \frac{1}{\sqrt{|S^1|}} (\mathbf{e}^{(1)})^\top \mathbf{C} \mathbf{U}_1 \mathbf{z} = 0. \tag{22}$$

The second condition in (22) demonstrates that for inequalities in (19) become equalities, $\mathbf{C}\mathbf{U}_1\mathbf{z}$ should lie in the orthogonal complement space of $\mathbf{e}^{(1)}$, which is spanned by \mathbf{U}_1 . Therefore, if the second condition in (22) is satisfied, there exists a vector $\mathbf{b} \in \mathbb{R}^{N-1}$ such that:

$$\mathbf{C}\mathbf{U}_1\mathbf{z} = \mathbf{U}_1\mathbf{b}. \quad (23)$$

In this case, the first condition in (22) becomes:

$$\mathbf{U}_1^\top \mathbf{C}\mathbf{U}_1\mathbf{z} = \mathbf{U}_1^\top \mathbf{U}_1\mathbf{b} = \mathbf{I}_{N-1}\mathbf{b} = \mathbf{b} = \eta\mathbf{z} \quad (24)$$

Therefore, the following equality should hold to meet both criterion in (20):

$$\mathbf{C}\mathbf{U}_1\mathbf{z} = \mathbf{U}_1\mathbf{b} = \eta\mathbf{U}_1\mathbf{z}. \quad (25)$$

(25) demonstrates that the conditions in (20) are met, if $\mathbf{U}_1\mathbf{z}$ is the eigenvector of $\mathbf{C} = \mathbf{Q}^\top\mathbf{Q}$ associated with eigenvalue η . This eigenvector $\mathbf{U}_1\mathbf{z}$ lies in the orthogonal complement space of $\mathbf{e}^{(0)}$ and the eigenvector of $\mathbf{C} = \mathbf{Q}^\top\mathbf{Q}$ is the right singular vector of \mathbf{Q} . Therefore, inequalities in (19) become equalities, if there is a right singular vector $\boldsymbol{\alpha}$ of \mathbf{Q} such that $(\mathbf{e}^{(1)})^\top\boldsymbol{\alpha} = 0$, which concludes the proof.

\mathbf{A} is created in the following way:

$$\mathbf{A} = \begin{bmatrix} \mathbf{U}_{sub}^\top \mathbf{C}\mathbf{U}_{sub} & \frac{1}{\sqrt{|S^0|}} \mathbf{U}_{sub}^\top \mathbf{C}(\mathbf{e}^{(0)}) \\ \frac{1}{\sqrt{|S^0|}} (\mathbf{e}^{(0)})^\top \mathbf{C}\mathbf{U}_{sub} & \frac{1}{|S^0|} (\mathbf{e}^{(0)})^\top \mathbf{C}\mathbf{e}^{(0)} \end{bmatrix}, \quad (26)$$

together with eigenvalues $\eta_1 \leq \dots \leq \eta_{N-1}$. Furthermore, (16) shows that $\mathbf{U}_{sub}^\top \mathbf{C}\mathbf{U}_{sub} \in \mathbb{R}^{N-2 \times N-2}$ has the eigenvalues $0 \leq \gamma_1^2 \leq \dots \leq \gamma_{N-2}^2$. Again, we can apply Cauchy interlace theorem presented in Lemma 2, which concludes that:

$$\eta_1 \leq \gamma_1^2 \leq \eta_2 \leq \gamma_2^2 \leq \dots \leq \gamma_{N-2}^2 \leq \eta_{N-1}, \quad (27)$$

where $\eta_i = \gamma_i^2$ or $\eta_i = \gamma_{i-1}^2$, if and only if there is a right singular vector $\boldsymbol{\alpha}$ of \mathbf{Q} such that $(\mathbf{e}^{(0)})^\top\boldsymbol{\alpha} = 0$ and $(\mathbf{e}^{(1)})^\top\boldsymbol{\alpha} = 0$. For these conditions leading to equalities $\eta_i = \gamma_i^2$ or $\eta_i = \gamma_{i-1}^2$, the proof follows in the same manner as the previous one.

Finally, by unifying the results of (19) and (27), the Theorem 1 can be proved, such that:

$$\lambda_1 \leq \gamma_1 \quad (28)$$

$$\lambda_2 \leq \gamma_2 \quad (29)$$

$$\vdots$$

$$\lambda_{N-2} \leq \gamma_{N-2} \leq \lambda_N \quad (30)$$

where $\lambda_i = \gamma_i$ or $\lambda_N = \gamma_{N-2}$, only if \mathbf{Q} have a right singular vector $\boldsymbol{\alpha}$ such that $(\mathbf{e}^{(0)})^\top\boldsymbol{\alpha} = 0$ and $(\mathbf{e}^{(1)})^\top\boldsymbol{\alpha} = 0$. Note that λ_i s and γ_i s are defined to be non-negative, thus we can omit the powers of 2 in the final result.

B Learning Environment and Proof for Theorem 1

We first introduce the following Lemma that will be utilized in the proof.

Lemma 3. (Theorem 1, [51]) Let $\mathbf{x}_1, \dots, \mathbf{x}_N \sim \mathcal{N}(\mathbf{0}, \boldsymbol{\Sigma})$ be independent Gaussian vectors, where $\boldsymbol{\Sigma}$ is an $F \times F$ real positive definite matrix. Let \mathbf{B} be a fixed symmetric real $N \times N$ matrix. Consider the compound Wishart matrix $\mathbf{W} = \mathbf{X}\mathbf{B}\mathbf{X}^\top/N$ with $\mathbf{X} = [\mathbf{x}_1, \dots, \mathbf{x}_N]$. Then for any $\delta \geq 0$, the following event

$$\|\mathbf{W} - \mathbb{E}\mathbf{W}\|_2 \geq \frac{32\|\mathbf{B}\|_F\delta + 64\|\mathbf{B}\|_2\delta^2}{N} \|\boldsymbol{\Sigma}\|_2$$

holds with probability at most $2 \exp(-2\delta^2 + 2F \log 3)$, where $\|\cdot\|_F$ denotes the Frobenius norm. Specifically, for $\delta \geq \sqrt{2 \ln(3)}\sqrt{F}$,

$$\|\mathbf{W} - \mathbb{E}\mathbf{W}\|_2 \geq \frac{32\|\mathbf{B}\|_F\delta + 64\|\mathbf{B}\|_2\delta^2}{N} \|\boldsymbol{\Sigma}\|_2$$

holds with probability at most $2 \exp(-\delta^2)$.

Model: For the node classification task over a graph \mathcal{G} , a linear one-layer GNN-based model is considered, where the models without and with individual shifts for different sensitive groups are denoted by $f^{vanilla}(\mathbf{X}, \mathbf{Q}) = \mathbf{w}^\top \mathbf{XQ}$ and $f^{MShift}(\mathbf{X}, \mathbf{Q}) = \mathbf{w}^\top \mathbf{XQN}^{(0)}\mathbf{N}^{(1)}$, respectively. Note that $\mathbf{w} \in \mathbb{R}^{F \times 1}$, $\mathbf{X} \in \mathbb{R}^{F \times N}$ and $\mathbf{Q} \in \mathbb{R}^{N \times N}$.

Training loss: Let $\mathbf{Z}^{vanilla} \in \mathbb{R}^{F \times N}$ and $\mathbf{Z}^{MShift} \in \mathbb{R}^{F \times N}$ denote \mathbf{XQ} and $\mathbf{XQN}^{(0)}\mathbf{N}^{(1)}$, respectively. The training loss for both the models without and with individual shifts for different sensitive groups follows as:

$$\mathcal{L}(\mathbf{w}) = \frac{1}{2} \|\mathbf{Z}^\top \mathbf{w} - \mathbf{y}\|_2^2 \quad (31)$$

where $\mathbf{y} \in \mathbb{R}^N$ denotes the labels of the nodes. Note that this loss is applicable to both $\mathbf{Z}^{vanilla}$ and \mathbf{Z}^{MShift} , and \mathbf{Z} is used interchangeably with $\mathbf{Z}^{vanilla}$ for the ease of notation.

Optimization: Gradient descent is utilized for the optimization by initializing $\mathbf{w}_0 = \mathbf{0}$, where an optimization step can be written as:

$$\begin{aligned} \mathbf{w}_{t+1} &= \mathbf{w}_t - \eta(\mathbf{ZZ}^\top \mathbf{w}_t - \mathbf{Zy}) \\ &= (\mathbf{I}_F - \eta\mathbf{ZZ}^\top) \mathbf{w}_t + \eta\mathbf{Zy}. \end{aligned} \quad (32)$$

Note that η in Equation (32) denotes the learning rate.

In this setting, \mathbf{w}_t converges to optimal solution $\mathbf{w}^* = (\mathbf{ZZ}^\top)^\dagger \mathbf{Zy}$ according to the solution of least squares problem [50], where superscript \dagger denotes Moore-Penrose inverse. The residual of \mathbf{w}_{t+1} follows as:

$$\begin{aligned} \mathbf{w}_{t+1} - \mathbf{w}^* &= (\mathbf{I}_F - \eta\mathbf{ZZ}^\top) \mathbf{w}_t + \eta\mathbf{Zy} - \mathbf{w}^* \\ &= (\mathbf{I}_F - \eta\mathbf{ZZ}^\top) \mathbf{w}_t + \eta(\mathbf{ZZ}^\top)(\mathbf{ZZ}^\top)^\dagger \mathbf{Zy} - \mathbf{w}^* \\ &= (\mathbf{I}_F - \eta\mathbf{ZZ}^\top) \mathbf{w}_t - (\mathbf{I}_F - \eta\mathbf{ZZ}^\top) \mathbf{w}^*, \text{ as } \mathbf{w}^* = (\mathbf{ZZ}^\top)^\dagger \mathbf{Zy} \\ &= (\mathbf{I}_F - \eta\mathbf{ZZ}^\top) (\mathbf{w}_t - \mathbf{w}^*). \end{aligned} \quad (33)$$

Assumption 1: $\mathbf{w}_0 = \mathbf{0}$.

Based on Assumption 1 and (33), following inequality can be written:

$$\|\mathbf{w}_t - \mathbf{w}^*\| \leq \|(\mathbf{I}_F - \eta\mathbf{ZZ}^\top)\|^t \|\mathbf{w}^*\|. \quad (34)$$

For the learning rate $\eta = \frac{1}{\sigma_{max}(\mathbf{ZZ}^\top)}$, the following convergence rate can be guaranteed for this problem:

$$\|\mathbf{w}_t - \mathbf{w}^*\| \leq \left(1 - \frac{\sigma_{min}(\mathbf{ZZ}^\top)}{\sigma_{max}(\mathbf{ZZ}^\top)}\right)^t \|\mathbf{w}^*\|. \quad (35)$$

Note that σ_{min} and σ_{max} output the minimum and maximum positive eigenvalues of the input matrix, respectively. The same result can also be derived for \mathbf{Z}^{MShift} following the same steps, such as:

$$\|\mathbf{w}_t - \mathbf{w}^*\| \leq \left(1 - \frac{\sigma_{min}(\mathbf{Z}^{MShift}(\mathbf{Z}^{MShift})^\top)}{\sigma_{max}(\mathbf{Z}^{MShift}(\mathbf{Z}^{MShift})^\top)}\right)^t \|\mathbf{w}^*\|. \quad (36)$$

Equations (35) and (36) demonstrate that the convergence rates of the defined node classification problem for without and with shifts depend on the terms $1 - \left(\frac{\sigma_{min}(\mathbf{ZZ}^\top)}{\sigma_{max}(\mathbf{ZZ}^\top)}\right)$ and $1 - \left(\frac{\sigma_{min}(\mathbf{Z}^{MShift}(\mathbf{Z}^{MShift})^\top)}{\sigma_{max}(\mathbf{Z}^{MShift}(\mathbf{Z}^{MShift})^\top)}\right)$, respectively. Therefore, the next step examines these factors together with the following assumptions.

Assumption 2: $\mathbf{x} \in \mathbb{R}^F$ is a centered Gaussian random variable with covariance matrix $\Sigma = \mathbb{E}_x[\mathbf{x}\mathbf{x}^\top]$. The features of nodes $\mathbf{x}_1, \dots, \mathbf{x}_N$ are independent realizations of \mathbf{x} , where $\mathbf{X} = [\mathbf{x}_1 \cdots \mathbf{x}_N]$. $\mathbf{Z} = \mathbf{XQ}$ and $\mathbf{Z}^{MShift} = \mathbf{XQN}^{(0)}\mathbf{N}^{(1)}$.

Assumption 3: $\mathbb{E}[\mathbf{XQ}] := \mathbf{Y}$.

Assumption 4: $\mathbf{O} \preceq \mathbb{E}\left[\frac{(\mathbf{XQ} - \mathbf{Y})(\mathbf{XQ} - \mathbf{Y})^\top}{\sqrt{N}}\right] \preceq \delta_1 \mathbf{I}_F$

Assumption 5: $\mathbf{O} \preceq \mathbb{E}\left[\frac{(\mathbf{XQ} - \mathbf{Y})\mathbf{N}^{(0)}\mathbf{N}^{(1)}(\mathbf{XQ} - \mathbf{Y})^\top}{\sqrt{N}}\right] \preceq \delta_1 \mathbf{I}_F$

Assumption 6: Defined \mathbf{Y} matrix is full rank.

We will analyze the eigenvalues of $\frac{1}{N}\mathbf{Z}\mathbf{Z}^\top$, as multiplying with a constant does not change the ratio between the minimum and maximum eigenvalues.

$$\frac{1}{N}\mathbf{Z}\mathbf{Z}^\top = \frac{1}{N} \sum_{i=1}^N \mathbf{z}_i \mathbf{z}_i^\top. \quad (37)$$

For the analysis of $\frac{1}{N}\mathbf{Z}\mathbf{Z}^\top$, we will first focus on $\mathbb{E} \left[\frac{\mathbf{Z}\mathbf{Z}^\top}{N} \right]$, which equals to:

$$\begin{aligned} \mathbb{E} \left[\frac{\mathbf{Z}\mathbf{Z}^\top}{N} \right] &= \mathbb{E} \left[\frac{\mathbf{X}\mathbf{Q}}{\sqrt{N}} \left(\frac{\mathbf{X}\mathbf{Q}}{\sqrt{N}} \right)^\top \right] \\ &= \frac{\mathbf{Y}\mathbf{Y}^\top}{N} + \mathbb{E} \left[\frac{(\mathbf{X}\mathbf{Q} - \mathbf{Y})}{\sqrt{N}} \frac{(\mathbf{X}\mathbf{Q} - \mathbf{Y})^\top}{\sqrt{N}} \right] \end{aligned} \quad (38)$$

based on the Assumption 3. By utilizing Weyl's inequality and the provided assumptions, following inequalities can be written:

$$\begin{aligned} \sigma_{\max} \left(\frac{\mathbf{Y}\mathbf{Y}^\top}{N} \right) &\leq \sigma_{\max} \left(\mathbb{E} \left[\frac{\mathbf{Z}\mathbf{Z}^\top}{N} \right] \right) \leq \sigma_{\max} \left(\frac{\mathbf{Y}\mathbf{Y}^\top}{N} \right) + \delta_1 \\ \sigma_{\min} \left(\frac{\mathbf{Y}\mathbf{Y}^\top}{N} \right) &\leq \sigma_{\min} \left(\mathbb{E} \left[\frac{\mathbf{Z}\mathbf{Z}^\top}{N} \right] \right) \leq \sigma_{\min} \left(\frac{\mathbf{Y}\mathbf{Y}^\top}{N} \right) + \delta_1 \end{aligned} \quad (39)$$

Similarly:

$$\begin{aligned} \mathbb{E} \left[\frac{\mathbf{Z}^{MShift}(\mathbf{Z}^{MShift})^\top}{N} \right] &= \mathbb{E} \left[\frac{\mathbf{X}\mathbf{Q}\mathbf{N}^{(0)}\mathbf{N}^{(1)}(\mathbf{X}\mathbf{Q}\mathbf{N}^{(0)}\mathbf{N}^{(1)})^\top}{\sqrt{N}\sqrt{N}} \right] \\ &= \mathbb{E} \left[\frac{\mathbf{X}\mathbf{Q}}{\sqrt{N}} (\mathbf{N}^{(0)}\mathbf{N}^{(1)})^2 \frac{(\mathbf{X}\mathbf{Q})^\top}{\sqrt{N}} \right], \text{ as } \mathbf{N}^{(0)}\mathbf{N}^{(1)} \text{ commutes,} \\ &= \mathbb{E} \left[\frac{\mathbf{X}\mathbf{Q}}{\sqrt{N}} \mathbf{N}^{(0)}\mathbf{N}^{(1)} \frac{(\mathbf{X}\mathbf{Q})^\top}{\sqrt{N}} \right], \text{ as } \mathbf{N}^{(0)}\mathbf{N}^{(1)} \text{ is a projection matrix} \\ &= \frac{\mathbf{Y}\mathbf{N}^{(0)}\mathbf{N}^{(1)}\mathbf{Y}^\top}{N} + \mathbb{E} \left[\frac{(\mathbf{X}\mathbf{Q} - \mathbf{Y})}{\sqrt{N}} \mathbf{N}^{(0)}\mathbf{N}^{(1)} \frac{(\mathbf{X}\mathbf{Q} - \mathbf{Y})^\top}{\sqrt{N}} \right] \end{aligned} \quad (40)$$

Again, by utilizing Weyl's inequality and the provided assumptions, following inequalities can be written for the shifted case:

$$\begin{aligned} \sigma_{\max} \left(\frac{\mathbf{Y}\mathbf{N}^{(0)}\mathbf{N}^{(1)}\mathbf{Y}^\top}{N} \right) &\leq \sigma_{\max} \left(\mathbb{E} \left[\frac{\mathbf{Z}^{MShift}(\mathbf{Z}^{MShift})^\top}{N} \right] \right) \leq \sigma_{\max} \left(\frac{\mathbf{Y}\mathbf{N}^{(0)}\mathbf{N}^{(1)}\mathbf{Y}^\top}{N} \right) + \delta_1 \\ \sigma_{\min} \left(\frac{\mathbf{Y}\mathbf{N}^{(0)}\mathbf{N}^{(1)}\mathbf{Y}^\top}{N} \right) &\leq \sigma_{\min} \left(\mathbb{E} \left[\frac{\mathbf{Z}^{MShift}(\mathbf{Z}^{MShift})^\top}{N} \right] \right) \leq \sigma_{\min} \left(\frac{\mathbf{Y}\mathbf{N}^{(0)}\mathbf{N}^{(1)}\mathbf{Y}^\top}{N} \right) + \delta_1 \end{aligned} \quad (41)$$

Next step in the proof is bounding the errors $\left\| \frac{1}{N}\mathbf{Z}\mathbf{Z}^\top - \mathbb{E} \left[\frac{\mathbf{Z}\mathbf{Z}^\top}{N} \right] \right\|_2$ and $\left\| \frac{1}{N}\mathbf{Z}^{MShift}(\mathbf{Z}^{MShift})^\top - \mathbb{E} \left[\frac{\mathbf{Z}^{MShift}(\mathbf{Z}^{MShift})^\top}{N} \right] \right\|_2$. Based on Lemma 3 and assumption 2, the following inequality holds with probability $1 - \epsilon$, where $\epsilon < \frac{2}{e}$, for errors $\left\| \frac{1}{N}\mathbf{Z}\mathbf{Z}^\top - \mathbb{E} \left[\frac{\mathbf{Z}\mathbf{Z}^\top}{N} \right] \right\|_2$ and $\left\| \frac{1}{N}\mathbf{Z}^{MShift}(\mathbf{Z}^{MShift})^\top - \mathbb{E} \left[\frac{\mathbf{Z}^{MShift}(\mathbf{Z}^{MShift})^\top}{N} \right] \right\|_2$:

$$\left\| \frac{1}{N}\mathbf{Z}\mathbf{Z}^\top - \mathbb{E} \left[\frac{\mathbf{Z}\mathbf{Z}^\top}{N} \right] \right\|_2 \leq \mathcal{O} \left(\frac{\log(2/\epsilon)}{N} \right), \quad (42)$$

where the constants $\|\mathbf{Q}\mathbf{Q}^\top\|_F$, $\|\mathbf{Q}\mathbf{Q}^\top\|_2$, and $\|\Sigma\|_2$ are hidden in $\mathcal{O}(\cdot)$ notation for a focus on N , similar to the approach taken in [26]. Similarly, the following bound holds for $\left\|\frac{1}{N}\mathbf{Z}^{MShift}(\mathbf{Z}^{MShift})^\top - \mathbb{E}\left[\frac{\mathbf{Z}^{MShift}(\mathbf{Z}^{MShift})^\top}{N}\right]\right\|_2$ with probability $1 - \epsilon$, where $\epsilon < \frac{2}{e}$:

$$\left\|\frac{1}{N}\mathbf{Z}^{MShift}(\mathbf{Z}^{MShift})^\top - \mathbb{E}\left[\frac{\mathbf{Z}^{MShift}(\mathbf{Z}^{MShift})^\top}{N}\right]\right\|_2 \leq \mathcal{O}\left(\frac{\log(2/\epsilon)}{N}\right). \quad (43)$$

Based on Lemma 3, Equations (42) and (43), the inequalities in (39) and (41) can be re-organized. Following inequalities hold with probability $1 - \epsilon$ where $\epsilon < \frac{2}{e}$:

$$\sigma_{max}\left(\frac{\mathbf{Y}\mathbf{Y}^\top}{N}\right) - \mathcal{O}\left(\frac{\log(2/\epsilon)}{N}\right) \leq \sigma_{max}\left(\frac{\mathbf{Z}\mathbf{Z}^\top}{N}\right) \leq \sigma_{max}\left(\frac{\mathbf{Y}\mathbf{Y}^\top}{N}\right) + \delta_1 + \mathcal{O}\left(\frac{\log(2/\epsilon)}{N}\right) \quad (44)$$

$$\sigma_{min}\left(\frac{\mathbf{Y}\mathbf{Y}^\top}{N}\right) - \mathcal{O}\left(\frac{\log(2/\epsilon)}{N}\right) \leq \sigma_{min}\left(\frac{\mathbf{Z}\mathbf{Z}^\top}{N}\right) \leq \sigma_{min}\left(\frac{\mathbf{Y}\mathbf{Y}^\top}{N}\right) + \delta_1 + \mathcal{O}\left(\frac{\log(2/\epsilon)}{N}\right)$$

$$\begin{aligned} \sigma_{max}\left(\frac{\mathbf{Y}\mathbf{N}^{(0)}\mathbf{N}^{(1)}\mathbf{Y}^\top}{N}\right) - \mathcal{O}\left(\frac{\log(2/\epsilon)}{N}\right) &\leq \sigma_{max}\left(\frac{1}{N}\mathbf{Z}^{MShift}(\mathbf{Z}^{MShift})^\top\right) \\ &\leq \sigma_{max}\left(\frac{\mathbf{Y}\mathbf{N}^{(0)}\mathbf{N}^{(1)}\mathbf{Y}^\top}{N}\right) + \delta_1 + \mathcal{O}\left(\frac{\log(2/\epsilon)}{N}\right) \end{aligned}$$

$$\begin{aligned} \sigma_{min}\left(\frac{\mathbf{Y}\mathbf{N}^{(0)}\mathbf{N}^{(1)}\mathbf{Y}^\top}{N}\right) - \mathcal{O}\left(\frac{\log(2/\epsilon)}{N}\right) &\leq \sigma_{min}\left(\frac{1}{N}\mathbf{Z}^{MShift}(\mathbf{Z}^{MShift})^\top\right) \\ &\leq \sigma_{min}\left(\frac{\mathbf{Y}\mathbf{N}^{(0)}\mathbf{N}^{(1)}\mathbf{Y}^\top}{N}\right) + \delta_1 + \mathcal{O}\left(\frac{\log(2/\epsilon)}{N}\right) \end{aligned} \quad (45)$$

By the same method that proves Theorem 1 and is presented in Appendix A, it can be shown that positive eigenvalues of $\mathbf{Y}\mathbf{N}^{(0)}\mathbf{N}^{(1)}\mathbf{Y}^\top$ are interlaced between the positive eigenvalues of $\mathbf{Y}\mathbf{Y}^\top$:

$$\sigma_{min}(\mathbf{Y}\mathbf{Y}^\top) \leq \sigma_{min}(\mathbf{Y}\mathbf{N}^{(0)}\mathbf{N}^{(1)}\mathbf{Y}^\top) \leq \sigma_{max}(\mathbf{Y}\mathbf{N}^{(0)}\mathbf{N}^{(1)}\mathbf{Y}^\top) \leq \sigma_{max}(\mathbf{Y}\mathbf{Y}^\top) \quad (46)$$

where inequalities become equalities, only if there is a right singular vector α of \mathbf{Y}^\top that is orthogonal to both $\mathbf{e}^{(0)}$ and $\mathbf{e}^{(1)}$.

Assumption 7: None of the right singular vector of \mathbf{Y}^\top is orthogonal to both $\mathbf{e}^{(0)}$ and $\mathbf{e}^{(1)}$

Based on Assumption 7 and result in (46), following holds:

$$\sigma_{min}\left(\frac{\mathbf{Y}\mathbf{Y}^\top}{N}\right) < \sigma_{min}\left(\frac{\mathbf{Y}\mathbf{N}^{(0)}\mathbf{N}^{(1)}\mathbf{Y}^\top}{N}\right) < \sigma_{max}\left(\frac{\mathbf{Y}\mathbf{N}^{(0)}\mathbf{N}^{(1)}\mathbf{Y}^\top}{N}\right) < \sigma_{max}\left(\frac{\mathbf{Y}\mathbf{Y}^\top}{N}\right) \quad (47)$$

Finally, for small enough δ_1 and large enough N with probability $1 - \epsilon$ with $\epsilon < \frac{2}{e}$, the following inequalities can be written:

$$\begin{aligned} \sigma_{min}\left(\frac{1}{N}\mathbf{Z}\mathbf{Z}^\top\right) &\leq \sigma_{min}\left(\frac{\mathbf{Y}\mathbf{Y}^\top}{N}\right) + \delta_1 + \mathcal{O}\left(\frac{\log(2/\epsilon)}{N}\right) \\ &< \sigma_{min}\left(\frac{\mathbf{Y}\mathbf{N}^{(0)}\mathbf{N}^{(1)}\mathbf{Y}^\top}{N}\right) - \mathcal{O}\left(\frac{\log(2/\epsilon)}{N}\right) \\ &\leq \sigma_{min}\left(\frac{1}{N}\mathbf{Z}^{MShift}(\mathbf{Z}^{MShift})^\top\right) \\ &\leq \sigma_{max}\left(\frac{1}{N}\mathbf{Z}^{MShift}(\mathbf{Z}^{MShift})^\top\right) \\ &\leq \sigma_{max}\left(\frac{\mathbf{Y}\mathbf{N}^{(0)}\mathbf{N}^{(1)}\mathbf{Y}^\top}{N}\right) + \delta_1 + \mathcal{O}\left(\frac{\log(2/\epsilon)}{N}\right) \\ &< \sigma_{max}\left(\frac{\mathbf{Y}\mathbf{Y}^\top}{N}\right) - \mathcal{O}\left(\frac{\log(2/\epsilon)}{N}\right) \\ &\leq \sigma_{max}\left(\frac{1}{N}\mathbf{Z}\mathbf{Z}^\top\right) \end{aligned} \quad (48)$$

Therefore, Equation (48) proves that $1 - \left(\frac{\sigma_{\min}(\mathbf{Z}\mathbf{Z}^\top)}{\sigma_{\max}(\mathbf{Z}\mathbf{Z}^\top)}\right) > 1 - \left(\frac{\sigma_{\min}(\mathbf{Z}^{MShift}(\mathbf{Z}^{MShift})^\top)}{\sigma_{\max}(\mathbf{Z}^{MShift}(\mathbf{Z}^{MShift})^\top)}\right)$ with probability $1 - \epsilon$. Unifying this result with Equations (35) and (36) concludes that shifted model by matrices $\mathbf{N}^{(0)}\mathbf{N}^{(1)}$ converges faster compared to the vanilla model with high probability in the considered learning environment for node classification.

C Proof of Theorem 2

Define the sample mean after normalization layer by $\bar{\boldsymbol{\mu}}^{(n)} \in \mathbb{R}^F$, $n = 0, 1$. Then,

$$\begin{aligned}\|\bar{\boldsymbol{\mu}}^{(0)} - \bar{\boldsymbol{\mu}}^{(1)}\| &= \left\| \frac{1}{|\mathcal{S}^0|} \sum_{j \in \mathcal{S}^0} \bar{\mathbf{h}}_j^{(0)} - \frac{1}{|\mathcal{S}^1|} \sum_{j \in \mathcal{S}^1} \bar{\mathbf{h}}_j^{(1)} \right\| \\ \|\boldsymbol{\mu}^{(0)} - \boldsymbol{\mu}^{(1)}\| &= \left\| \frac{1}{|\mathcal{S}^0|} \sum_{j \in \mathcal{S}^0} \text{Act}(\bar{\mathbf{h}}_j^{(0)}) - \frac{1}{|\mathcal{S}^1|} \sum_{j \in \mathcal{S}^1} \text{Act}(\bar{\mathbf{h}}_j^{(1)}) \right\|_1.\end{aligned}\tag{49}$$

We can write $\bar{\mathbf{h}}_j^{(0)} = \bar{\boldsymbol{\mu}}^{(0)} + \bar{\boldsymbol{\delta}}_j^{(0)}$, $\forall j = 1 \dots |\mathcal{S}^0|$ and $\bar{\mathbf{h}}_j^{(1)} = \bar{\boldsymbol{\mu}}^{(1)} + \bar{\boldsymbol{\delta}}_j^{(1)}$, $\forall j = 1 \dots |\mathcal{S}^1|$. If the activation function $\text{Act}(\cdot)$ is Lipschitz continuous with Lipschitz constant L (applies to several nonlinear activations, such as rectified linear unit (ReLU), sigmoid), the following holds:

$$\begin{aligned}\text{Act}(\bar{\boldsymbol{\mu}}_i^{(0)}) - L|\bar{\boldsymbol{\delta}}_{i,j}^{(0)}| &\leq \text{Act}(\bar{\mathbf{h}}_{i,j}^{(0)}) = \text{Act}(\bar{\boldsymbol{\mu}}_i^{(0)} + \bar{\boldsymbol{\delta}}_{i,j}^{(0)}) \\ &\leq \text{Act}(\bar{\boldsymbol{\mu}}_i^{(0)}) + L|\bar{\boldsymbol{\delta}}_{i,j}^{(0)}|, \forall i = 1, \dots, F \\ \text{Act}(\bar{\boldsymbol{\mu}}^{(0)}) - L|\bar{\boldsymbol{\delta}}_j^{(0)}| &\preceq \text{Act}(\bar{\mathbf{h}}_j^{(0)}) = \text{Act}(\bar{\boldsymbol{\mu}}^{(0)} + \bar{\boldsymbol{\delta}}_j^{(0)}) \\ &\preceq \text{Act}(\bar{\boldsymbol{\mu}}^{(0)}) + L|\bar{\boldsymbol{\delta}}_j^{(0)}|, \forall j = 1, \dots, |\mathcal{S}^0|\end{aligned}\tag{50}$$

where $|\cdot|$ takes the element-wise absolute value of the input. The same inequalities can also be written for \mathcal{S}^1 :

$$\begin{aligned}\text{Act}(\bar{\boldsymbol{\mu}}^{(1)}) - L|\bar{\boldsymbol{\delta}}_j^{(1)}| &\preceq \text{Act}(\bar{\mathbf{h}}_j^{(1)}) = \text{Act}(\bar{\boldsymbol{\mu}}^{(1)} + \bar{\boldsymbol{\delta}}_j^{(1)}) \preceq \text{Act}(\bar{\boldsymbol{\mu}}^{(1)}) + L|\bar{\boldsymbol{\delta}}_j^{(1)}|, \\ &\forall j = 1, \dots, |\mathcal{S}^1|\end{aligned}\tag{51}$$

Based on Equations (49), (50), and (51), following holds:

$$\begin{aligned}\frac{1}{|\mathcal{S}^0|} \sum_{j \in \mathcal{S}^0} \left(\text{Act}(\bar{\boldsymbol{\mu}}^{(0)}) - L|\bar{\boldsymbol{\delta}}_j^{(0)}| \right) - \frac{1}{|\mathcal{S}^1|} \sum_{j \in \mathcal{S}^1} \left(\text{Act}(\bar{\boldsymbol{\mu}}^{(1)}) + L|\bar{\boldsymbol{\delta}}_j^{(1)}| \right) &\preceq \boldsymbol{\mu}^{(0)} - \boldsymbol{\mu}^{(1)} \\ &\preceq \frac{1}{|\mathcal{S}^0|} \sum_{j \in \mathcal{S}^0} \left(\text{Act}(\bar{\boldsymbol{\mu}}^{(0)}) + L|\bar{\boldsymbol{\delta}}_j^{(0)}| \right) - \frac{1}{|\mathcal{S}^1|} \sum_{j \in \mathcal{S}^1} \left(\text{Act}(\bar{\boldsymbol{\mu}}^{(1)}) - L|\bar{\boldsymbol{\delta}}_j^{(1)}| \right)\end{aligned}\tag{52}$$

$$\begin{aligned}\text{Act}(\bar{\boldsymbol{\mu}}^{(0)}) - \text{Act}(\bar{\boldsymbol{\mu}}^{(1)}) - \frac{1}{|\mathcal{S}^0|} \sum_{j \in \mathcal{S}^0} L|\bar{\boldsymbol{\delta}}_j^{(0)}| - \frac{1}{|\mathcal{S}^1|} \sum_{j \in \mathcal{S}^1} L|\bar{\boldsymbol{\delta}}_j^{(1)}| &\preceq \boldsymbol{\mu}^{(0)} - \boldsymbol{\mu}^{(1)} \\ &\preceq \text{Act}(\bar{\boldsymbol{\mu}}^{(0)}) - \text{Act}(\bar{\boldsymbol{\mu}}^{(1)}) + \frac{1}{|\mathcal{S}^0|} \sum_{j \in \mathcal{S}^0} L|\bar{\boldsymbol{\delta}}_j^{(0)}| + \frac{1}{|\mathcal{S}^1|} \sum_{j \in \mathcal{S}^1} L|\bar{\boldsymbol{\delta}}_j^{(1)}|\end{aligned}\tag{53}$$

Define $\mathbf{a} := \text{Act}(\bar{\boldsymbol{\mu}}^{(0)}) - \text{Act}(\bar{\boldsymbol{\mu}}^{(1)}) - \frac{1}{|\mathcal{S}^0|} \sum_{j \in \mathcal{S}^0} L|\bar{\boldsymbol{\delta}}_j^{(0)}| - \frac{1}{|\mathcal{S}^1|} \sum_{j \in \mathcal{S}^1} L|\bar{\boldsymbol{\delta}}_j^{(1)}|$ and $\mathbf{b} := \text{Act}(\bar{\boldsymbol{\mu}}^{(0)}) - \text{Act}(\bar{\boldsymbol{\mu}}^{(1)}) + \frac{1}{|\mathcal{S}^0|} \sum_{j \in \mathcal{S}^0} L|\bar{\boldsymbol{\delta}}_j^{(0)}| + \frac{1}{|\mathcal{S}^1|} \sum_{j \in \mathcal{S}^1} L|\bar{\boldsymbol{\delta}}_j^{(1)}|$. Equation (53) leads to:

$$|\mu_i^{(0)} - \mu_i^{(1)}| \leq \max(|a_i|, |b_i|), \forall i = 1, \dots, F.\tag{54}$$

If we consider the case, $|a_i| \geq |b_i|$. Then:

$$\begin{aligned}
|\mu_i^{(0)} - \mu_i^{(1)}| &\leq \left| \text{Act}(\bar{\mu}_i^{(0)}) - \text{Act}(\bar{\mu}_i^{(1)}) - \frac{1}{|\mathcal{S}^0|} \sum_{j \in \mathcal{S}^0} L|\bar{\delta}_{j,i}^{(0)}| - \frac{1}{|\mathcal{S}^1|} \sum_{j \in \mathcal{S}^1} L|\delta_{j,i}^{(1)}| \right| \\
&\leq \left| \text{Act}(\bar{\mu}_i^{(0)}) - \text{Act}(\bar{\mu}_i^{(1)}) \right| + \left| \frac{1}{|\mathcal{S}^0|} \sum_{j \in \mathcal{S}^0} L|\bar{\delta}_{j,i}^{(0)}| \right| + \left| \frac{1}{|\mathcal{S}^1|} \sum_{j \in \mathcal{S}^1} L|\bar{\delta}_{j,i}^{(1)}| \right| \\
&\leq \left| \text{Act}(\bar{\mu}_i^{(0)}) - \text{Act}(\bar{\mu}_i^{(1)}) \right| + L \left| \bar{\Delta}_i^{(0)} \right| + L \left| \bar{\Delta}_i^{(1)} \right|,
\end{aligned} \tag{55}$$

where $\bar{\Delta}_i^{(0)} := \max_j |\bar{\delta}_{j,i}^{(0)}|$ and $\bar{\Delta}_i^{(1)} := \max_j |\bar{\delta}_{j,i}^{(1)}|$.

Consider the term $\text{Act}(\bar{\mu}_i^{(0)}) - \text{Act}(\bar{\mu}_i^{(1)})$:

$$\text{Act}(\bar{\mu}_i^{(0)}) - \text{Act}(\bar{\mu}_i^{(1)}) = \text{Act}(\bar{\mu}_i^{(0)} + \bar{\mu}_i^{(1)} - \bar{\mu}_i^{(1)}) - \text{Act}(\bar{\mu}_i^{(1)}). \tag{56}$$

Utilizing Equations (50) and (51), $\text{Act}(\bar{\mu}_i^{(0)} + \bar{\mu}_i^{(1)} - \bar{\mu}_i^{(1)}) - \text{Act}(\bar{\mu}_i^{(1)})$ can be bounded by below and above:

$$\begin{aligned}
\text{Act}(\bar{\mu}_i^{(1)}) - L|\bar{\mu}_i^{(0)} - \bar{\mu}_i^{(1)}| - \text{Act}(\bar{\mu}_i^{(1)}) &\leq \text{Act}(\bar{\mu}_i^{(0)} + \bar{\mu}_i^{(1)} - \bar{\mu}_i^{(1)}) - \text{Act}(\bar{\mu}_i^{(1)}) \\
&\leq \text{Act}(\bar{\mu}_i^{(1)}) + L|\bar{\mu}_i^{(0)} - \bar{\mu}_i^{(1)}| - \text{Act}(\bar{\mu}_i^{(1)})
\end{aligned} \tag{57}$$

$$-L|\bar{\mu}_i^{(0)} - \bar{\mu}_i^{(1)}| \leq \text{Act}(\bar{\mu}_i^{(0)} + \bar{\mu}_i^{(1)} - \bar{\mu}_i^{(1)}) - \text{Act}(\bar{\mu}_i^{(1)}) \leq L|\bar{\mu}_i^{(0)} - \bar{\mu}_i^{(1)}| \tag{58}$$

$$\left| \text{Act}(\bar{\mu}_i^{(0)}) - \text{Act}(\bar{\mu}_i^{(1)}) \right| \leq L|\bar{\mu}_i^{(0)} - \bar{\mu}_i^{(1)}| \tag{59}$$

Therefore:

$$|\mu_i^{(0)} - \mu_i^{(1)}| \leq L|\bar{\mu}_i^{(0)} - \bar{\mu}_i^{(1)}| + L \left| \bar{\Delta}_i^{(0)} \right| + L \left| \bar{\Delta}_i^{(1)} \right|, \forall i \text{ such that } |a_i| \geq |b_i|. \tag{60}$$

Next step is to consider the case, $|a_i| < |b_i|$. For this case, following inequalities hold:

$$\begin{aligned}
|\mu_i^{(0)} - \mu_i^{(1)}| &\leq \left| \text{Act}(\bar{\mu}_i^{(0)}) - \text{Act}(\bar{\mu}_i^{(1)}) + \frac{1}{|\mathcal{S}^0|} \sum_{j \in \mathcal{S}^0} L|\bar{\delta}_{j,i}^{(0)}| + \frac{1}{|\mathcal{S}^1|} \sum_{j \in \mathcal{S}^1} L|\bar{\delta}_{j,i}^{(1)}| \right| \\
&\leq \left| \text{Act}(\bar{\mu}_i^{(0)}) - \text{Act}(\bar{\mu}_i^{(1)}) \right| + \left| \frac{1}{|\mathcal{S}^0|} \sum_{j \in \mathcal{S}^0} L|\bar{\delta}_{j,i}^{(0)}| \right| + \left| \frac{1}{|\mathcal{S}^1|} \sum_{j \in \mathcal{S}^1} L|\bar{\delta}_{j,i}^{(1)}| \right| \\
&\leq \left| \text{Act}(\bar{\mu}_i^{(0)}) - \text{Act}(\bar{\mu}_i^{(1)}) \right| + L \left| \bar{\Delta}_i^{(0)} \right| + L \left| \bar{\Delta}_i^{(1)} \right| \\
&\leq L|\bar{\mu}_i^{(0)} - \bar{\mu}_i^{(1)}| + L \left| \bar{\Delta}_i^{(0)} \right| + L \left| \bar{\Delta}_i^{(1)} \right|, \forall i \text{ such that } |a_i| \geq |b_i|.
\end{aligned} \tag{61}$$

Combining Equations (60) and (61), the following inequality can be written:

$$|\mu_i^{(0)} - \mu_i^{(1)}| \leq L|\bar{\mu}_i^{(0)} - \bar{\mu}_i^{(1)}| + L \left| \bar{\Delta}_i^{(0)} \right| + L \left| \bar{\Delta}_i^{(1)} \right|, \forall i = 1, \dots, F. \tag{62}$$

which concludes:

$$\|\boldsymbol{\mu}^{(0)} - \boldsymbol{\mu}^{(1)}\| \leq L \left(\|\bar{\boldsymbol{\mu}}^{(0)} - \bar{\boldsymbol{\mu}}^{(1)}\| + \|\bar{\boldsymbol{\Delta}}^{(0)}\| + \|\bar{\boldsymbol{\Delta}}^{(1)}\| \right). \tag{63}$$

D Additional Statistics on Datasets

Table 2 presents further statistical information on the utilized datasets. In the table, $\|\mathcal{S}_0\|$ and $\|\mathcal{S}_1\|$ are the cardinalities of the sets of nodes with sensitive attributes 0 and 1, respectively. 'Inter-edges' and 'Intra-edges' correspond to the number of edges linking nodes from different sensitive groups and the same sensitive group, respectively. F in Table 2 denotes the dimension of nodal features.

Table 2: Dataset statistics

Dataset	$\ \mathcal{S}_0\ $	$\ \mathcal{S}_1\ $	Inter-edges	Intra-edges	F
Pokec-z	4851	2808	1140	28336	59
Pokec-n	4040	2145	943	20901	59
Recidivism	9317	9559	298098	325642	17

E Hyperparameters

We provide the selected hyperparameter values for the GNN model and the proposed framework for the reproducibility of the presented results. In the GNN-based classifier, weights are initialized utilizing Glorot initialization [52]. All models are trained for 1000 epochs by employing Adam optimizer [45] together with a learning rate of 10^{-3} and ℓ_2 weight decay factor of 10^{-5} . A 2-layer GCN network followed by a linear layer is employed for node classification. Hidden dimension of the node representations is selected as 64 on all datasets.

The results for baseline schemes, covariance, adversarial, HTR_{DDP} regularizers, and FairGNN [12] are obtained by choosing corresponding hyperparameters (the multiplying factors for these regularizers in the overall loss) via grid search on cross-validation sets with 5 different data splits. Specifically, a grid search on the values $10^9, 10^{10}, 10^{11}$ is executed for covariance-based regularizer. Furthermore, the values 0.01, 0.1, 1.10 are examined as the multiplier for adversarial regularizer. FairGNN employs both covariance-based and adversarial regularizers, therefore its parameter selection is the unification of the previous two hyperparameter selection methods. Finally, the parameters 0.01, 0.1, 1, 10 are examined for the HTR_{DDP} regularizer.

Hyperparameter values for the proposed FairNorm whose results are presented in Section 5.2 can be found in Table 3. These parameters are selected via grid search on cross-validation sets over 5 different data splits. The range of the parameters are selected based on the corresponding loss terms. Specifically, the values 10, 100, 1000 values are examined for κ in Pokec networks, and the values 0.01, 0.1, 1 values are examined for κ in Recidivism network. After the selection of best κ value, the τ is selected together with the fixed, best κ value. While the values $10^{-7}, 10^{-8}, 10^{-9}, 10^{-10}$ values are examined for τ in Pokec networks, the values $10^{-8}, 10^{-9}, 10^{-10}, 10^{-11}$ values are examined for κ in Recidivism network

Table 3: Utilized κ and τ values for the presented results in Table 1

ReLU	Pokec-z	Pokec-n	Recidivism
κ/τ	100/ 10^{-7}	1000/ 10^{-9}	0.01/ 10^{-10}
Sigmoid	Pokec-z	Pokec-n	Recidivism
κ/τ	10/ 10^{-7}	100/ 10^{-8}	0.01/ 10^{-10}

F Sensitivity Analysis

In order to examine the effects of hyperparameter selection, the sensitivity analysis for the proposed framework is executed. The results for changing κ and τ values are presented in Tables 4 and 5 for Pokec networks and Recidivism network, respectively. Overall, the results demonstrate that the proposed strategy, FairNorm, typically leads to better fairness measures compared to the natural baseline (M-Norm) within a wide range of hyperparameter selection.

G Ablation Study

In order to investigate the influences of different fairness regularizers introduced in this study, we carry over an ablation study. The results of this study are presented in Table 6. Table 6 demonstrates that while the employment of \mathcal{L}_μ seems to have a greater effect in fairness performance improvement,

Table 4: Sensitivity Analysis for Pokec Networks

ReLU	Pokec-z			Pokec-n		
	Acc (%)	Δ_{SP} (%)	Δ_{EO} (%)	Acc (%)	Δ_{SP} (%)	Δ_{EO} (%)
M-Norm	70.71 \pm 0.8	5.57 \pm 1.3	5.00 \pm 2.0	69.25 \pm 0.5	2.48 \pm 1.2	2.91 \pm 1.7
$\tau = 10^{-8}, \kappa = 10$	70.26 \pm 0.9	1.52 \pm 1.0	2.19 \pm 1.2	69.45 \pm 0.6	2.23 \pm 1.3	2.65 \pm 1.6
$\tau = 10^{-8}, \kappa = 100$	70.48 \pm 0.9	1.40 \pm 1.0	2.20 \pm 1.2	69.53 \pm 0.8	2.07 \pm 1.0	1.98 \pm 0.8
$\tau = 10^{-8}, \kappa = 1000$	70.37 \pm 1.1	3.20 \pm 0.9	3.18 \pm 2.0	69.38 \pm 0.8	1.55 \pm 1.4	1.48 \pm 1.7
$\kappa = 100, \tau = 10^{-7}$	70.67 \pm 1.0	1.35 \pm 1.2	1.90 \pm 1.8	69.56 \pm 0.8	2.10 \pm 0.9	2.09 \pm 0.5
$\kappa = 100, \tau = 10^{-8}$	70.48 \pm 0.9	1.40 \pm 1.0	2.20 \pm 1.7	69.53 \pm 0.8	2.07 \pm 1.0	1.98 \pm 0.8
$\kappa = 100, \tau = 10^{-9}$	70.55 \pm 0.9	1.48 \pm 1.2	1.99 \pm 1.8	69.54 \pm 0.7	2.15 \pm 1.1	1.84 \pm 0.9

Sigmoid	Pokec-z			Pokec-n		
	Acc (%)	Δ_{SP} (%)	Δ_{EO} (%)	Acc (%)	Δ_{SP} (%)	Δ_{EO} (%)
M-Norm[26]	69.84 \pm 0.7	6.21 \pm 1.4	4.44 \pm 2.1	68.59 \pm 0.9	1.78 \pm 2.1	2.88 \pm 1.8
$\tau = 10^{-8}, \kappa = 10$	69.71 \pm 0.9	1.36 \pm 0.4	1.72 \pm 1.1	68.97 \pm 0.8	2.23 \pm 1.3	2.49 \pm 1.8
$\tau = 10^{-8}, \kappa = 100$	70.05 \pm 1.2	1.19 \pm 0.8	2.53 \pm 1.0	68.88 \pm 1.1	1.44 \pm 1.2	1.74 \pm 1.7
$\tau = 10^{-8}, \kappa = 1000$	70.06 \pm 1.1	1.17 \pm 0.7	2.47 \pm 1.3	68.37 \pm 0.7	2.21 \pm 1.1	3.47 \pm 1.8
$\kappa = 100, \tau = 10^{-7}$	70.06 \pm 1.2	1.28 \pm 0.8	2.39 \pm 1.2	68.87 \pm 1.1	1.45 \pm 1.2	1.85 \pm 1.6
$\kappa = 100, \tau = 10^{-8}$	70.05 \pm 1.2	1.19 \pm 0.8	2.53 \pm 1.0	68.88 \pm 1.1	1.44 \pm 1.2	1.74 \pm 1.7
$\kappa = 100, \tau = 10^{-9}$	70.06 \pm 1.2	1.20 \pm 0.8	2.53 \pm 1.0	68.81 \pm 1.1	1.70 \pm 1.2	1.90 \pm 1.7

Table 5: Sensitivity Analysis for Recidivism Network

Recidivism	ReLU			Sigmoid		
	Acc (%)	Δ_{SP} (%)	Δ_{EO} (%)	Acc (%)	Δ_{SP} (%)	Δ_{EO} (%)
M-Norm	95.00 \pm 0.3	8.87 \pm 1.2	1.71 \pm 0.7	94.45 \pm 0.3	8.94 \pm 1.2	2.06 \pm 1.0
$\tau = 10^{-10}, \kappa = 1$	95.01 \pm 0.2	8.76 \pm 1.2	1.66 \pm 0.6	94.38 \pm 0.2	7.27 \pm 1.0	0.95 \pm 1.0
$\tau = 10^{-10}, \kappa = 0.1$	95.02 \pm 0.3	8.62 \pm 1.1	1.43 \pm 0.5	94.27 \pm 0.3	7.29 \pm 1.1	0.89 \pm 1.0
$\tau = 10^{-10}, \kappa = 0.01$	95.11 \pm 0.2	8.45 \pm 1.0	0.90 \pm 0.5	94.32 \pm 0.2	7.28 \pm 1.1	0.80 \pm 0.9
$\kappa = 0.1, \tau = 10^{-9}$	94.99 \pm 0.2	8.59 \pm 1.1	1.17 \pm 0.6	94.33 \pm 0.3	7.39 \pm 1.1	1.12 \pm 1.0
$\kappa = 0.1, \tau = 10^{-10}$	95.02 \pm 0.3	8.62 \pm 1.1	1.43 \pm 0.5	94.27 \pm 0.3	7.29 \pm 1.1	0.89 \pm 1.0
$\kappa = 0.1, \tau = 10^{-11}$	94.98 \pm 0.1	8.48 \pm 1.1	1.32 \pm 1.0	94.38 \pm 0.2	7.27 \pm 1.0	1.14 \pm 1.1

utilization of both \mathcal{L}_μ and \mathcal{L}_Δ (FairNorm) leads to better fairness results compared to the cases where only one of the regularizers is used with ReLU activation. For the case where sigmoid is used as the nonlinear activation, use of both regularizers again results in better Δ_{EO} values compared to the cases where only one of the regularizers is employed. However, the same cannot be always claimed for Δ_{SP} , which can be explained by the fact that sigmoid already limits the maximal deviation to some extent after the first layer reducing the effect of \mathcal{L}_Δ . Overall, Table 6 shows that the utilization of both \mathcal{L}_μ and \mathcal{L}_Δ generally achieves the best fairness performance, while \mathcal{L}_μ appears to be a more influential component compared to \mathcal{L}_Δ for the bias reduction.

Table 6: Ablation study for the proposed regularizers

ReLU	Pokec-z			Pokec-n			Recidivism		
	Accuracy (%)	Δ_{SP} (%)	Δ_{EO} (%)	Accuracy (%)	Δ_{SP} (%)	Δ_{EO} (%)	Accuracy (%)	Δ_{SP} (%)	Δ_{EO} (%)
M-Norm[26]	70.71 \pm 0.8	5.57 \pm 1.3	5.00 \pm 2.0	69.25 \pm 0.5	2.48 \pm 1.2	2.91 \pm 1.7	95.00 \pm 0.3	8.87 \pm 1.2	1.71 \pm 0.7
\mathcal{L}_μ	70.65 \pm 0.8	1.50 \pm 1.0	2.19 \pm 1.3	69.30 \pm 0.7	1.47 \pm 1.2	1.51 \pm 1.4	95.08 \pm 0.2	8.67 \pm 1.0	1.35 \pm 0.5
\mathcal{L}_Δ	70.62 \pm 0.9	5.15 \pm 1.4	4.55 \pm 2.2	69.40 \pm 0.5	2.55 \pm 1.1	2.54 \pm 1.6	95.12 \pm 0.2	8.97 \pm 1.1	1.42 \pm 0.6
FairNorm	70.67 \pm 1.0	1.35 \pm 1.2	1.90 \pm 1.8	69.38 \pm 0.7	1.26 \pm 1.2	1.22 \pm 1.3	95.11 \pm 0.2	8.45 \pm 1.0	0.90 \pm 0.5

Sigmoid	Pokec-z			Pokec-n			Recidivism		
	Accuracy (%)	Δ_{SP} (%)	Δ_{EO} (%)	Accuracy (%)	Δ_{SP} (%)	Δ_{EO} (%)	Accuracy (%)	Δ_{SP} (%)	Δ_{EO} (%)
M-Norm[26]	69.84 \pm 0.7	6.21 \pm 1.4	4.44 \pm 2.1	68.59 \pm 0.9	1.78 \pm 2.1	2.88 \pm 1.8	94.45 \pm 0.3	8.94 \pm 1.2	2.06 \pm 1.0
\mathcal{L}_μ	69.71 \pm 0.9	1.36 \pm 0.4	1.72 \pm 1.1	68.82 \pm 1.1	1.65 \pm 1.2	1.80 \pm 1.8	94.33 \pm 0.2	7.18 \pm 1.2	1.05 \pm 1.1
\mathcal{L}_Δ	69.73 \pm 0.5	5.67 \pm 2.0	4.29 \pm 2.3	68.59 \pm 0.9	1.78 \pm 2.1	2.88 \pm 1.8	94.39 \pm 0.3	8.81 \pm 1.1	1.92 \pm 0.9
FairNorm	69.73 \pm 0.9	1.71 \pm 0.3	1.48 \pm 1.1	68.88 \pm 1.1	1.44 \pm 1.2	1.74 \pm 1.7	94.32 \pm 0.2	7.28 \pm 1.1	0.80 \pm 0.9

H Computing Infrastructures

Software infrastructures: All GNN-based models are trained utilizing PyTorch 1.10.2 [53] and NetworkX 2.6.3 [54].

Hardware infrastructures: Experiments are carried over on a server with 4 NVIDIA RTX A4000 GPUs and 32 AMD Ryzen Threadripper 3970X CPUs.